Earth-Science Reviews
October 2021, Volume 221, Pages 103754 (21p.)
https://doi.org/10.1016/j.earscirev.2021.103754
https://archimer.ifremer.fr/doc/00710/82158/

Volcanological evolution of Montagne Pelée (Martinique): A textbook case of alternating Plinian and dome-forming eruptions

Boudon Georges [1], Balcone-Boissard Hélène [2, *]

[1] Université de Paris, Institut de physique du globe de Paris, CNRS, F-75005 Paris, France
[2] ISTeP - Sorbonne Université, CNRS, UMR 7193, 75005 Paris, France

* Corresponding author : Hélène Balcone-Boissard, email address :
helene.balcone_boissard@sorbonne-universite.fr

Abstract :

Montagne Pelée is one of the most active volcanoes of the Lesser Antilles arc, with two to three magmatic eruptions per millennium and an estimated magmatic production rate in the order of 0.7 km3/1000 years. Montagne Pelée is also infamous for the very large number of people (30000) killed by an eruptive phenomenon at the onset of the 1902–1905 dome-forming eruption. Active for ~550 kyrs, Montagne Pelée has undergone two major flank collapses that influenced its volcanological as well as magmatic evolution. The last one occurred at around 36 ka. Due to changes in the threshold effect following the decrease in load of the volcanic edifice due to flank collapse, there was a switch in emitted magma from generally andesitic to basaltic andesites. After 10 kyrs of intense activity, the load exerted by the new edifice once again prevented dense basaltic andesite magma from reaching the surface, whereas andesitic magmas, similar to the initial ones, continued to be emitted. All the magmas come from a common magma ponding zone at 200 ± 50 MPa, 875 ± 25 °C, an oxygen fugacity (fO2) between 0.4 and 0.8 log unit above the nickel-nickel oxide (NNO) oxygen buffer, and melt H2O contents of 5.3–6.3 wt%. Based on comparative on-land and marine tephrochronological studies, we have reconstructed a detailed eruptive history of the volcano over the last 25 kyrs. The volcano produced a succession of Plinian-SubPlinian and dome-forming eruptions, making it a textbook case for studying this duality, which sometimes occurred during a single eruption. We identified more than 55 magmatic eruptions, with a ratio of 2/3 for dome-forming vs. Plinian eruptions. An unusual feature of this volcano is that dome-forming eruptions often start with violent, superficial and laterally directed explosions. These generate highly devastating dilute and turbulent pyroclastic density currents on the southwestern and southern flanks of the volcano, as illustrated by the seven events of this type during the first months of the 1902–1905 eruption. On the basis of the past eruptions over the last millennia, a series of scenarios can be proposed in the event of reactivation, including no magmatic eruption, a phreatic event or a magmatic eruption (Plinian or dome-forming eruption, with or without an explosive phase).

Keywords : Montagne Pelée (Martinique, Lesser Antilles), Flank-collapse, Magma, Plinian eruption, Dome-forming eruption

1. Introduction

Subduction volcanoes are the most abundant emerged volcanoes on Earth. Their activity is highly dependent on the subduction rate: high subduction rates result in a high partial melting rate of the mantle wedge above the subducting lithosphere, leading to a high magma production rate and a high eruptive frequency, sometimes with very large-volume eruptions (km^3 to tens of km^3). This is the case of most of the volcanoes of the Pacific "Ring of Fire", where the subduction rate can reach more than 10 cm/year (DeMets et al., 2010). Conversely, when the subduction rate is slow, the magma volume and the eruptive frequency of the volcanoes are lower: this is the case for the Lesser Antilles arc where the subduction rate of the North and South Atlantic plates beneath the small Caribbean plate is of the order of 2 cm/year (Wadge, 1984). Magmas at subduction zones commonly result from a mixture of diverse sources that may include the subducting slab with its fluids, the mantle wedge, and the crust through which the melt ascends (Davidson, 1987; McCulloch and Gamble, 1991). They show widespread compositions ranging from basalts to rhyolites, most of them belonging to the calc-alkaline series (Gill, 1981), intermediate magmas (basaltic andesites, andesites) are the most abundant compared to basalts and more evolved magmas such as dacites and rhyolites. Magmas are thus rather silica-rich, but also volatile-rich (Eichelberger, 1995; Cassidy et al., 2018), giving rise to diverse eruptions, from effusive to highly explosive. The most frequent eruptive styles are vulcanian to subPlinian or Plinian eruptions and lava dome-forming eruptions. In addition, it is not rare to observe a shift in eruptive styles during an eruption (hereafter designated as multi-style) because of a small change in composition (through emission of different parts of a stratified magma reservoir or different lenses of melt in a transcrustal plumbing system) or changes in magma flux, due to a transition of the degassing regime within the conduit during ascent of a magma of constant composition

(Woods and Koyaguchi, 1994; Martel et al., 1998; Villemant and Boudon, 1998; Degruyter and Bonadonna, 2012), or magmatic gas flushing (Caricchi et al., 2007; Gonnermann and Manga, 2007; Cassidy et al., 2018; Caricchi et al., 2018). In addition, significant modifications to the volcano's shape through flank collapses (Lesser Antilles, Boudon et al., 2007; 2013; Mount St Helens: Voight et al., 1981; Bezymianny 1956: Belousov, 1996; Shiveluch 1964: Belousov, 1995) may also generate changes in eruptive styles, by modifying the load pressure on the plumbing system. In the last few decades, there have been several eruptions worldwide of this multi-style type such as Mount St. Helens (USA, 1980-1986) (Christiansen and Peterson, 1981) and Soufrière Hills (Montserrat, 1995-2010) (Sparks and Young, 2002).

The existence of a duality between the two end-member eruptive styles (Plinian-SubPlinian vs. lava dome-forming) is common in subduction zones. Understanding magma behaviour during these two contrasted eruptive styles is essential in terms of risk assessment and for the protection of the populations that live on the flanks of such volcanoes. Montagne Pelée (Martinique), in the Lesser Antilles arc, offers a good opportunity to shed light on this duality: the succession of these two eruptive styles over the last tens of thousands of years has been systematically detailed. Numerous works have been carried out on this volcano combining on-land and offshore studies. The eruptive history has been established by on-land studies (Roobol and Smith, 1976; Westercamp and Traineau, 1983a, b; Smith and Roobol, 1990; Germa et al., 2011a, 2015; Boudon et al., 2005; Michaud-Dubuy et al., 2019) supplemented by tephrochronological studies on marine cores collected during oceanographic cruises (Boudon et al., 2013; Solaro et al., 2020). The structure of the volcano has been approached by studying flank-collapses combining on-land and offshore investigations (Vincent et al., 1989; Le Friant et al., 2003, 2015; Boudon et al., 2007; Brunet et al., 2015). Petrological investigations have been performed on eruptive products (Traineau et al., 1983;

Bourdier et al., 1985; Dupuy et al., 1985; Fichaut, 1986; Fichaut et al., 1989a, b; Gourgaud et al, 1989; Smith and Roobol, 1990; Martel et al., 1998; Pichavant et al., 2002). Detailed studies on selected eruptions, including dome-forming (Lacroix, 1904; Perret, 1937; Fisher et al., 1980; Fisher and Heiken 1982; Boudon and Lajoie, 1989; Bourdier et al., 1989; Lajoie et al., 1989; Tanguy, 1994, 2004; Villemant and Boudon., 1998; Boudon et al., 2015) and Plinian or sub-Plinian eruptions (Bardintzeff et al., 1989; Traineau et al., 1989; Balcone-Boissard et al., 2010; Carazzo et al., 2012, 2019, 2020; Michaud-Dubuy, 2019; Michaud-Dubuy et al., 2019) have also been carried out.

Here, the objective is to synthetize the numerous works dealing with Montagne Pelée to propose a complete updated panorama of the volcano's evolution, including its structure, its volcanological history and its magmatics. Such a synthesis provides useful constraints on other volcanic systems in subduction zones. Moreover, we can use these data to improve our knowledge in the event of reactivation and for volcanic crisis management.

2. Montagne Pelée in the Lesser Antilles arc

Montagne Pelée is located in the northern part of Martinique Island in the Lesser Antilles arc (Fig. 1a), one of the two subduction arcs bordering the Atlantic Ocean, the other being the Sandwich Islands arc. It results from the oblique subduction of the northern and southern Atlantic plates under the Caribbean plate at a relatively slow rate of 2 cm/year (Wadge, 1984). The arc extends from 12° to 18° N with a marked convexity towards the East (Fig. 1a). Arc volcanism has been active since 40 Ma (Bouysse et al., 1990; Martin-Kaye, 1969). The nature of the crust on which the Lesser Antilles arc volcanoes are built is poorly known, though it potentially interacts with magmas during their ascent and storage. Davidson

and Harmon (1989) proposed that the whole arc is built on top of the accretionary prism of the former Aves volcanic arc. In addition, Larue et al. (1991) suggested that in the south, where the accretionary prism is the thickest, sediments overthrust the volcanic arc and form part of the crust. However, the extent of such overthrust fore-arc sediments is unclear and these features have not been described north of St Lucia (Larue et al., 1991; Van Soest et al., 2002). Speed and Walker (1991) suggested that the southern part of the Lesser Antilles arc (from Dominica southward) is built on young oceanic crust produced by the opening of the Grenada Basin. Bouysse et al. (1990) proposed that only the northern part of the arc is built on an older volcanic arc belonging to the Aves system. Kopp et al. (2011) imaged the present island arc structure as a ~25 km thick crustal system, composed of three layers. A three-kilometer-thick upper crust of volcanogenic sedimentary and volcaniclastics rocks is underlained by an intermediate felsic middle crust and a plutonic lower crust. The island arc crust may comprise inherited elements of oceanic plateau material contributing to the observed crustal thickness. Xenoliths show considerable island-to-island variation in their petrology from plagioclase-free ultramafic lithologies to gabbros and gabbronorites with variable proportions of amphibole, indicative of changing magma differentiation depths (Melekhova et al., 2019). In addition to the Moho, a mid-crustal discontinuity is identified at about 10-25 km depth along the arc, with slightly deeper values in the north (Montserrat) as for the Moho (from 25 to 35 km depth south to north) (Schlaphorst et al., 2018).

Along the Lesser Antilles trench, the volcanic arc regionally shows a north-south dichotomy. North of Dominica, the arc is divided into two groups of islands. An older arc (Oligocene- early Miocene) is represented by the most easterly islands, on which the volcanoes are extinct, sometimes very eroded and covered by a thick carbonate platform (Fig. 1a). Active volcanoes are located on the islands of the western part, which represent the recent arc whose construction began around 20 Ma (Bouysse et al., 1990). This has been interpreted

as a migration of the volcanism (Pichot, 2012 ; Legendre et al., 2018). The origin of this split into two distinct arcs is debated. The peculiar curvature of the Lesser Antilles trench has been acquired since the Paleocene subsequent to the entrance of the buoyant Bahamas Bank in the Greater Antilles subduction zone. This event locked the subduction process, triggering the plate boundary reorganization, cessation, and migration of the arc in the forearc of the subduction zone. Since the late Oligocene-early Miocene, the volcanic arc of the Lesser Antilles shows a peculiar feature; south of Martinique, the arc emplaced and stayed in a rather steady-state position and the volcanic activity was continuous and slightly migrated westward (less than 10 km, i.e., the width of the island) whereas north of this island, it ceased during the late Oligocene-early Miocene interval and migrated westward to its present-day location. The duration of the volcanic hiatus is estimated to be approximately 10 Myr. South of Dominica, the two branches of the arc merge and the deposits of the older arc are frequently covered by those of the recent arc. The southern part of the arc is bordered to the West by the 3000 m-deep Grenada back-arc basin.

Twelve volcanoes are currently considered as active on the main islands of the recent arc. From north to south they are: Mount Misery (St Kitts), Nevis Peak (Nevis), Soufrière Hills (Montserrat), Soufrière (Guadeloupe), Morne Aux Diables, Morne Diablotin, Morne Trois Pitons-Micotrin and Morne Plat Pays Volcanic Complex (Dominica), Montagne Pelée (Martinique), Soufrière (St. Lucia), Soufrière (St. Vincent) and Kick'em Jenny (Grenada). Martinique is the sole island in the arc that shows an across-arc distribution of volcanic formations belonging to the old and recent arcs without juxtaposition, whereas on all the other islands of the southern part of the arc products from the recent arc generally cover the older ones (Westercamp et al., 1989; Germa et al., 2011a). Thus, volcanic formations can be observed with a migration of the activity from the Oligocene (25 Ma) to present from the

southeast to the northwest of the island. Montagne Pelée, located in the northern part of the island, is the only active volcano on Martinique (Figs. 1b, c, 2).

3. Structure and volcanic evolution of Montagne Pelée

Montagne Pelée is one of the most active volcanoes in the Lesser Antilles arc. For several decades it was considered that Montagne Pelée was located between two older volcanoes (Fig. 2a). To the south is the Morne Jacob - Pitons du Carbet system, whose activity ended around 320 ka ago (Samper et al., 2008; Germa et al, 2010) with a large flank collapse (Fig. 1b), allowing the build-up of steep lava domes made of highly-crystallized and viscous magmas (Boudon et al., 2013), while to the north is Mont Conil. Germa et al. (2011b) proposed on the basis of a series of K-Ar ages that the activity of Mont Conil ranges from 550 to 126 ka, representing a more recent activity than proposed in older works (Nagle et al., 1976; Westercamp et al., 1989). Consequently, the first half of Mont Conil edification was contemporaneous with the activity of Pitons du Carbet over a period of ~250 ka. Progressively the magma production stopped in the south and became focused in the north beneath Mont Conil, generating abundant lava flows and lava domes leading to a volcano with a probable minimum height of 1050 m. Mont Conil's activity stopped 127 ka ago (Germa et al., 2011b, 2015) following a large flank collapse called "The Prêcheur event" that destroyed the southwestern flank of the volcano (Le Friant et al., 2003; Boudon et al., 2007). The age of the flank collapse is derived from two K-Ar ages obtained on pre- and post-collapse magmatic samples: 127 ± 2 ka on a pre-collapse lava flow and 126 ± 2 ka on a lava dome (Piton Marcel) located on the rim of the flank collapse (Fig. 2a) but inside the horseshoe-shaped structure and thus corresponding to post collapse activity (Germa et al., 2011b). These two lava samples have very close geochemical compositions, as do all magmas

from Mont Conil and Montagne Pelée (Labanieh et al., 2010; Germa et al., 2011b), suggesting a common magmatic system feeding both volcanic centers (Fig. 3). This has led to the hypothesis that Mont Conil is not independent of Montagne Pelée but can be considered as the primitive Montagne Pelée (first stage of edification), destroyed by the Le Prêcheur flank collapse. Considering the geometry and size of the flank-collapse structure, the summit area of this primitive volcanic edifice was probably located not far from the summit of the present Montagne Pelée cone, but with a larger extension than that of the present-day Mont Conil area (Fig. 2a). The collapse volume of the " Le Prêcheur event" was first estimated at 25 km^3 and the resulting horseshoe-shaped structure around 8 x 6 km (Le Friant et al., 2003). More recently, Germa et al. (2015) proposed a lower volume of 14.7 km^3 obtained on the basis of a geomorphological model of evolution of the volcano. Most of the debris avalanche flowed into the sea a part from an on-land one kilometer-long piece of the flank (Morne Julien, Fig. 2a), considered as a large hummock, partially covered by the products of more recent activity.

During the second stage of Montagne Pelée's activity, following the Prêcheur flank collapse, lava dome-forming eruptions and associated concentrated pyroclastic density currents (C-PDCs) were the dominant activity; such PDCs are highly concentrated gravity-driven flows of hot particles and gas. A new volcanic cone constructed which shows a well-defined asymmetry with steeper aerial and submarine slopes on the western flank compared to the eastern flank. Most of the pyroclastic deposits produced during this 2nd stage are indurated forming a succession of ridges particularly visible on the more eroded western flank (Figs 2a, b;). The emitted magmas are dominantly andesites (Fig 3).

The activity of the last tens of thousands of years and the resulting deposits have been well studied by on-land and offshore investigations, with diverse interpretations. A first scenario proposed the occurrence of two flank collapses in the last 25 kyrs (Le Friant et al., 2003): namely the "St. Pierre" and the "Rivière Sèche" events. The St. Pierre flank collapse

was estimated to have formed a 6 x 4 km horseshoe-shaped structure on-land intersecting the previously horseshoe-shaped structure and generating a second debris avalanche of 13 km^3 (8.8 km^3 following the model of Germa et al., 2015) that flowed into the sea in the Grenada basin. Based on geophysical surveys (seismic reflection, bathymetry, reflectivity), the Le Prêcheur and St. Pierre debris avalanche deposits (DAD) extend far into the Grenada Basin, reaching more than 50 km from the coast (Le Friant et al., 2003). The age of the second flank collapse was first estimated at 25 ka cal BP (^{14}C dating of on-land deposits within the horseshoe-shaped structure). Using stratigraphical and magmatic correlations between on-land deposits and tephra layers identified in a piston core (CAR-MAR 4 - Fig. 1b) drilled during the Caraval cruise northwest of Martinique, a new minimum age of 32 ka cal BP was proposed (Boudon et al., 2013). After this second flank collapse a new volcanic edifice grew, with deposits distributed both inside and outside the structure. A third flank collapse, called "The Rivière Sèche event" affected this new volcano. Of lower volume than the previous ones (2 to 3.5 ± 0.7 km^3, following the model of Le Friant et al. (2003) or Germa et al. (2015), respectively), it produced a horseshoe shaped structure (1.5 x 4 km) open toward the west and a debris avalanche that mainly flowed into the sea, stopping at the base of the submarine flank (Fig. 1b). Part of the debris avalanche remained on-land at the opening of the horseshoe-shaped structure, forming a series of small hills (Fig 2a). U-Th dating on the lava dome located inside the structure gives an age of ~9 ka for this event (Le Friant et al., 2003).

During the IODP Expedition 340, data were obtained from a series of marine cores off Montagne Pelée, which allow a new interpretation of the extent of the offshore DADs (Le Friant et al., 2015; Brunet et al., 2016): a large part of these deposits, with a chaotic seismic reflection signature, were initially interpreted as DADs, but in fact correspond to deformed sediments (named SLD – Fig 1b). Thus, the debris avalanche originating from the first flank collapse entered the sea, flowed over the submarine volcano slope, stopped and deposited

around the slope break forming the bulge observed in the bathymetry (Fig. 1b). This first - and largest - DAD weakened seafloor sediment due to its weight, and initiated seafloor sediment failure. Resulting submarine landslides propagated along a decollement surface, deforming in situ alternations of hemipelagic sediments and turbidity deposits (SLD, Fig. 1b). The DAD generated by the less voluminous second flank collapse may have locally remobilized sediments within the submarine landslide deposit, by exerting a normal stress that drove the deformation process. In addition, a core located on the submarine flank of Montagne Pelée (core U 1401A, 2590 mbsl) was drilled into what was interpreted as the third DAD resulting from the Rivière Sèche event (Fig. 1b). Although it was not possible to drill through it because of the heterogeneity of the deposit and the presence of large blocks (Le Friant et al., 2015), the pelagic sediments and volcanic deposits that covered the DAD were sampled. A detailed tephrochronological study combining ^{18}O stratigraphy and ^{14}C dating gives a minimum age of 36 ka for the emplacement of this DAD and thus of the associated flank collapse (Solaro et al., 2020). This new age together with the re-interpretation of the offshore deposits challenges several previous interpretations for the volcanic evolution of Montagne Pelée and the successive flank collapses.

A second scenario proposes the occurrence of only two flank collapses, as described by Solaro et al. (2020). While the morphology of the northern rim of the Le Prêcheur flank-collapse structure is clearly established, particularly by the hydrographic network and the distribution of the valleys on both sides of this rim, the southern rim is less clear, having been destroyed or covered by more recent products (Fig. 2b). The age of 127 ka obtained for two lava domes on the two sides of the rim is reliable (Germa et al., 2011a). The Rivière Sèche flank collapse is also clearly identified by the presence of submarine DADs, some remnants of hummock morphology on-land and the rims of the horseshoe-shaped structure (Le Friant et al., 2003). However, the occurrence of the St. Pierre flank collapse event is questionable for

several reasons : (i) the northern rim of this horseshoe-shaped structure is not clearly established, (ii) the distribution of the valleys coupled with the DEM underlines different orientations of the valleys within and outside the two flank-collapse structures (Fig. 2b), (iii) the DAD is also not clearly identified at the base of the submarine flank as it occurs intermixed with the first DAD in the same bulge (Brunet et al., 2016) and (iv) the time interval that separated the Le Prêcheur event (127 ka) and the Rivière Sèche event (≥36 ka) is around 90 ka. This time is short (considering a mean magma production rate of 0.6-0.7 km^3/1000 years, see discussion) to build an edifice which is then destroyed by a large flank collapse (St. Pierre), before the reconstruction of a new edifice, again destroyed by a new flank collapse (Rivière Sèche). This second scenario with only two flank collapses (Le Prêcheur and Rivière Sèche events) dated respectively at 127 and 36 ka is thus more likely (Fig. 2). In this new scenario, the Le Prêcheur flank-collapse structure is larger than previously proposed and its volume probably closer to or even greater than the volume initially proposed by Le Friant et al. (2003).

4. Montagne Pelée's history in the last 36 ka cal BP (3rd stage)

4.1. The volcanic activity during the period 36 - 25 ka cal BP

Following the last flank collapse (~36 ka), Montagne Pelée experienced numerous explosive eruptions involving less differentiated magmas than those emitted before (Figs. 3, 4, 5, 6, 7). There was an increase in the magma production, attested by the abundance of eruptive events : numerous marine tephra layers during the period up to 25 cal ky BP in the CAR-MAR 4 and U1401A cores (Boudon et al., 2013; Solaro et al., 2020 - Fig 7a, b, c), thick

low-silica pumice-rich (52-60% wt% SiO_2 - previously referred to as scoria) turbiditic deposits recognized in the U1401A core (Solaro et al., 2020; Fig 7b) and abundant on-land low-silica pumice-rich PDC deposits (Figs. 5, 6, 7d) (Traineau et al., 1983; Bourdier et al., 1985). These eruptions generated low-silica pumice PDCs by column collapse filling the horseshoe-shaped structure but also covering all the flanks of the growing volcano (Fig. 5). This activity occurred over approximatively 10 kyrs (i.e., ~36-25 ka), before decreasing progressively as shown by the decrease in the number of macroscopic tephra in the marine cores (Fig. 7b,c).

4.2. The activity between 25 ka cal BP and present

The preceding activity was followed by a renewal of the production of felsic magmas up to the present day (Figs. 3, 4). During this period, magmas covering the entire composition range found in Montagne Pelée were emitted (Fig. 3a, b), with the most felsic ones (SiO_2> 60 wt%) during the last magmatic eruptions of the last century (1902-1905, 1929-1932). Combined on-land and offshore data indicates that at least 55 eruptions occurred on Montagne Pelée (Figs. 6, 7). Plinian to subPlinian events and dome-forming eruptions were the two main eruptive styles, with 17 Plinian to subPlinian events and a minimum of 38 dome-forming eruptions (Fig. 7), including the two last historic eruptions (Roobol and Smith, 1976; Westercamp and Traineau, 1983a, b; Traineau et al., 1989; Smith and Roobol, 1990, Boudon et al., 2013; Solaro et al., 2020; Carazzo et al., 2012, 2019, 2020; Michaud Dubuy, 2019; Michaud Dubuy et al., 2019). Most of these eruptions have characteristics in common with the different historical and prehistorical eruptions described below.

4.3. The prehistoric activity of Montagne Pelée and the key eruptions

Written records of the historical volcanic activity of Montagne Pelée do not begin until after the arrival of the Europeans in 1635 (Du Tertre, 1654), although settlements were present on Martinique before that in the prehistoric period. Around 130 AD, the first Arawak Indians settled in northern Martinique from South America. They were decimated by the P2 Plinian eruption (now dated at 314 ± 69 AD; Fig. 6). Around 600 AD the Caribbean Indians, also originating from South America, settled on the island, exterminating the Arawak Indians. The Caribbean Indians experienced the last Plinian eruption of Montagne Pelée in 1348 ± 50 AD (P1 eruption), as shown by the numerous remains found at several sites at the base of pumice fallout deposits. They remained in Martinique for centuries after the P1 eruption, until the arrival of the Europeans in 1635, who killed them off.

- *The Plinian P3 eruption* (1929 ± 12 cal BP; 113 ± 85 AD) occurred probably just before the first settlement in Martinique. It was one of the most powerful Plinian eruptions of the recent period (1 km^3 of magma DRE, VE1 = 5, M = 5.4, Carazzo et al., 2020). It produced an eruptive column that reached a maximum height of 28-30 km generating a thick fallout pumice layer. Several collapses of the column produced a succession of PDCs channeled along the main valleys of the volcano, with an estimated volume of 0.7 km^3 DRE. The pumice fallout layers (0.3 km^3 DRE, Fig. 8a) are extensive, covering the whole flank of the volcano, and extending to the south onto the older volcano of the Pitons du Carbet with the 30 cm isopach located 15 km from the vent (Carazzo et al., 2020).

- *The Plinian P2 eruption* (1670 ± 32 cal BP; 394 ± 137 AD, Fig. 6), like the P3 eruption, produced a significant volume of magma (0.67-0.88 km^3 of magma DRE, VE1 = 4, M = 5.2) with the pumice fallout mainly found on the northeast flank of the volcano (Carazzo et al., 2019). The eruption started with the emplacement of a low-concentration PDC emplaced from a violent laterally directed blast to the northeast, followed by an eruptive

column that reached 23-26 km high, producing a pumice fallout that covered the northern flank of the volcano. This column partially collapsed several times, due to an increase in the mass eruption rate, and generated PDCs that were channeled along two main valleys on the southeast and northeast flanks of the volcano.

- A dome-forming eruption occurred at 884 ± 111 AD. Only a few deposits of diluted PDC (D-PDC) have been observed and dated from the western flank of the volcano (Smith and Roobol, 1990). As no deposit was preserved on the lower part of the volcano, it was probably an eruption of low intensity.

- *The P1 eruption* which occurred in 1348 ± 50 AD (624 ± 21 cal BP, Fig. 6) was a multi-style eruption (Villemant and Boudon, 1998). It began with a phreatic activity as attested by the centimeter-thick phreatic ash layer that covers the paleosoil on the western flank of the volcano (Fig. 8b). It was followed by two lapilli- and ash-D-PDCs (Figs. 8b, 9a) generated by superficial explosions in or at the base of a growing lava dome: the first one probably in the growing lava dome due to the low proportion of vesiculated clasts and the second one, probably immediately after, at the newly formed vent or in the higher part of the conduit as more vesiculated clasts are present. The depressurization of the conduit triggered a Plinian phase (Traineau et al., 1989; Bardintzeff et al.; 1989; Carazzo et al., 2012). This Plinian phase (VEI=4, M = 4.6) produced a high plume that reached a maximum height of 19-22 km, generating a pumice fallout layer covering principally the western flank of the volcano (Figs 8a, b, c, d). The partial collapse of the column generated PDCs channeled along a valley on the southwest flank of the volcano. The total volume of magma DRE emitted during the different phases of the eruption was in the order of 0.2 km^3.

- Another dome-forming eruption occurred in 1560 ± 80 AD. It was a dome-forming eruption of small intensity that generated only a few C-PDCs channeled in the Rivière des

Pères valley located on the southwestern flank of the volcano (Figs. 2, 5; Westercamp and Traineau, 1983a).

When the first Europeans settled in 1635 and founded the town of St. Pierre, they discovered a relief overhanging the bay devoid of vegetation; this was due to the last dome-forming eruption that had occurred a few decades earlier. They gave it the name of "Montagne Pelée" in reference to this unvegetated character.

4.4. The historical activity

During the historical period, the volcano erupted four times: first in 1792 and 1851 (minor phreatic eruptions), then in 1902-1905 and 1929-1932 (lava dome-forming eruptions preceded by minor phreatic outbursts).

4.4.1. The phreatic eruptions of 1792 and 1851

The 1792 eruption, which was of mild intensity, began in January and ended three months later. It produced block- and ash-fallout that contained old material and was limited in extent to the summit area (Figs 2a, 5). The 1851 eruption, between August and October, after four months of fumarolic activity, was more violent. Several phreatic explosions involving block- and ash-fallout destroyed the vegetation in the summit area and produced a fine ash which fell on the city of St. Pierre, 5 km away. The vents for these two eruptions were located below the summit crater on the upper western flank of the volcano (Fig. 1c).

4.4.2. The 1902-1905 dome-forming eruption

This is one of the most well-known historic eruptions in the world, described in detail by A. Lacroix in 1904. It can be divided into three main stages:

The pre-climactic stage: fumarolic activity was described inside the summit "Etang Sec" crater in 1889. But as there were no other observations of persistent fumarole activity until 1900, it is difficult to consider this as a precursor to the 1902 eruption. From the beginning of 1901, fumarolic activity appeared in the crater, and at the beginning of 1902 a marked increase was noticed, making it difficult to carry out human activity on the leeward side of the volcano (the west side of the volcano). On April 23, a first phreatic explosion occurred. During the following 15 days numerous phreatic events produced a thick ash layer on the western flank of the volcano and a much thinner layer over the city of St. Pierre. On May 5, a lahar generated by the destruction of a natural dam in the Etang Sec Crater (Fig. 2a) flowed down the Rivière Blanche towards its mouth killing 23 people in the Guerin factory, the first victims of the eruption. During the night of May 5, a glow was observed by the inhabitants of St. Pierre indicating that the magma had reached the surface inside the crater. During the night of May 7 - 8, a lahar in the Rivière du Prêcheur destroyed Le Prêcheur village causing the death of 400 people.

The climactic stage began on May 8 and ended on August 30, 1902. During this period seven violent and destructive turbulent D-PDCs destroyed the entire southwestern flank of the volcano (Figs. 2a, 8e, f, 9b). Among these explosions, four of them were particularly violent: May 8th, May 20th, June 6th and August 30th. The first one, on May 8th, partially destroyed the city of St. Pierre (Fig. 9b) and killed its 28,000 inhabitants (Figs. 8e, f, g). The last one, on August 30th, with a wider opening angle (~180°) destroyed part of the city of Morne Rouge located on the southern flank of the volcano (Fig. 2a) and killed 1500 people. The total number of victims of this eruption is therefore 30,000: this eruption has the sad record, worldwide and in historic times, of being directly responsible of the deaths of the largest

number of people by an eruptive phenomenon. Throughout this stage, the lava dome grew continuously inside the Etang Sec crater, being destroyed regularly by collapse of the unstable part of the lava dome or by superficial and low explosions, generating numerous block- and ash C-PDCs channeled down the Rivière Blanche valley (Fig. 8i) on the west side of the volcano (Lacroix, 1904; Tanguy, 2004). During this climatic stage, on July 9th, a vertical vulcanian explosion occurred on the lava dome; it probably generated some ash- and pumice-fallout, but the collapse of the vertical column also created an ash- and pumice-C-PDC that flowed in the Rivière Blanche valley. This event was described by Anderson and Flett (1903). Different interpretations have been proposed for the origin of the destructive and turbulent D-PDCs. Fisher et al. (1980) and Fisher and Heiken (1982) proposed that they originated from an ash-cloud surge separating from a block- and ash C-PDC flowing inside the Rivière Blanche valley and moving perpendicularly to the direction of the C-PDC. Bourdier et al. (1989), Boudon et al., (1989, 1990), Chadard and Lajoie (1989), Lajoie et al., (1989) offered an alternative interpretation based on a detailed field study. These D-PDCs resulted from laterally-directed explosions which occurred at the base of the growing lava dome in the Etang Sec crater with a wide opening angle (~120°). These D-PDCs were high-velocity, highly turbulent and dilute ground-hugging PDCs that expanded rapidly on the horizontal plane covering and devastating large areas on the southern and western flanks of the volcano (Fig. 9b). Their behavior, and the sedimentological characteristics of their deposits, are similar to those of the lateral blast from the 1980 Mount St. Helens eruption (Waitt et al., 1981). More recently, Gueugneau et al. (2020), based on numerical modeling, investigated the May 8th pyroclastic current by testing an ash-cloud surge generated by a block- and ash C-PDC flowing in the Rivière Blanche valley. They concluded that much of the distribution of the May 8th deposits, but not all the features, can be explained by an ash-cloud surge that separated early from a block- and ash C-PDC in the upper part of the volcano rather than in

the lower part of the Rivière blanche as proposed by Fisher and Heiken (1982). While this numerical model can partially explain the distribution of May 8thdeposits, it cannot explain the large distribution of the deposits from the August 30th event which had a larger opening angle (180°). The authors also suggest also that a blast-like event may be required at the initial stage of the explosion. So, we can consider that the laterally-directed explosions which occurred at the base of the growing lava dome are probably the best hypothesis to explain the distribution and features identified in the deposits generated by all these events.

The post climactic stage: from August 30th, 1902 to the beginning of 1905, the lava dome continued to grow (Fig. 8h) and numerous block- and ash C-PDCs partly filled the Rivière Blanche valley (Figs. 8i). This period was marked by the formation of several spines piercing the shell of the lava dome. The most spectacular was the growth between September 1902 and March 1903 of a large spine that reached a maximum a height of 350 m above the lava dome despite numerous collapses during its construction (Fig. 8j). Its estimated diameter of ~50 m gives an indication of the upper width of the feeding conduit. It was completely destroyed before the end of the eruption. This spine is the biggest ever observed in the world on a growing lava dome.

4.4.3. The 1929-1932 dome-forming eruption

After 24 years of fumarolic activity, a new eruption started in September 1929, described in detailed by F. Perret (1937). From August 1929, seismic tremors and an increase of the fumarolic activity were recorded. The first phreatic explosion occurred on September 16, 1929. The phreatic activity was intense until November, the probable date of the magma arrival at the surface. From 1929 to 1932 a new lava dome grew up inside the Etang Sec crater, and on the western part of the 1902-1905 lava dome, (Fig. 8h). The unstable areas of

this lava dome collapsed creating numerous block-and ash C-PDCs (Fig. 8k, l) which completely filled the Rivière Blanche valley (Fig. 8i). The accumulation of C-PDC deposits from the 1902-1905 and 1929-1932 eruptions exceeds 50 - 60 m in some places in the Rivière Blanche valley. No explosive activity, like that observed at the beginning of the 1902-1905 eruption, occurred.

4.4.4. The post-1932 activity

4.4.4.1. Hydrothermal activity. Following the 1929-1932 eruption, major degassing of the cooling lava dome continued for several years, before gradually decreasing and finally disappearing around 1970. Several thermo-mineral springs are present on the western flank of the volcano in different valleys but particularly in the high valley of Rivière Claire, and also along the coast (Barat, 1984). Most of the hydrothermal springs along the coast are resurgences of hydrothermal waters from the summit area flowing along the floor of the last flank-collapse structure of the volcano (Zlotnicki et al., 1998). Their temperatures range from ~ 30°C, to a maximum of ~70°C for Rivière Claire in the 1970's. They result from meteoric water that has been heated through conductive heat transfer at depth (equilibrium temperature of ~200-240 °C). The temperature of the different hot spring has progressively decreased to be now only at 32°C for the Rivière Claire hot spring.

4.4.4.2. Seismicity and landslides. Since the last magmatic eruption of 1929-1932, the volcanic seismicity beneath the active volcano has been very low. Two small crises have been recorded: a first one occurred in October-November 1980 and a second one between December 1985 and June 1986. During the 1980 crisis, 55 events were recorded in six days. This small crisis was correlated with the occurrence of an important landslide and associated

mud-flows; traces of this landslide were later found in the upper part of the Rivière du Prêcheur, near the summit area. Since the 1990s, numerous landslides have occurred in the upper part of this river, resulting from the instability of a cliff face made up mainly of pyroclastic products. These landslides create dammed lakes in the river that are regularly breached, generating lahars that can cause damage to the village of Le Prêcheur located at its mouth (Clouard et al., 2013; Aubaud et al., 2013).

In 1985-1986, 40 local events of very low magnitude and shallow depth were recorded beneath the southern rim of the Etang Sec crater (Hirn et al. 1987). In spite of the very low energy of these signals, these events were interpreted as very local and shallow variations in the effective stress of the hydrothermal system below the summit. From this period up to 2019, a few tens of events were recorded each year beneath the volcano. They were of very low magnitude (M<1) and of superficial origin (between 3 km below sea level and 1 km asl) resulting from the hydrothermal circulation. From April 2019, there has been increased seismicity, with a succession of seismic crises each comprising several tens of low magnitude events. They have all been located a few kilometers below the summit, and are related to perturbations in the hydrothermal system. In the last ten years, rare deeper (~10 km) seismic events have occurred, that are probably related to the magma plumbing system (http://www.ipgp.fr/fr/ovsm/bilans-trimestriels-de-lovsm).

5. Magmatology of Montagne Pelée's eruptive products

5.1. Typical calc-alkaline magmas

Montagne Pelée has emitted magmas with geochemical characteristics typical of island-arc calc-alkaline series (Figs. 3, 4, 10, 11 ; Traineau et al. 1983; Dupuy et al., 1985; Fichaut, 1986; Bourdier et al., 1989; Smith and Roobol, 1990; Villemant et al., 1996; Pichavant et al., 2002; Davidson and Wilson, 2010; Boudon et al., 2013; unpublished data), like all the volcanic centers from the recent arc in Martinique (Morne Jacob, Pitons du Carbet and Trois-Ilets volcanoes in the south; Smith and Roobol, 1990, Germa et al., 2011). Volcanic rocks from Montagne Pelée show a wide range of compositions, from basaltic andesites (i.e., SiO_2 > 52 wt%; alkali<4.5 wt%) to dacites (i.e., SiO_2 < 66 wt%; alkali < 5.5 wt%) with a lack of compositional gaps (Bourdier et al., 1985; Fichaut et al., 1989a; Gourgaud et al., 1989; Smith and Roobol, 1990). Some cumulates exhibit a picro-basaltic composition (i.e., SiO_2 between 39-46 wt %; alkali <2.5 wt%; Fig. 3). Nonetheless, the volcanic rocks are predominantly composed of andesites (57-63 wt% SiO_2; total alkali < 5 wt%); basaltic andesites and dacites are less common (Fig. 3) except for the time period after the last flank collapse when abundant low-silica pumice of basaltic andesite composition was erupted. CaO and Al_2O_3 contents are relatively high (6-10, 16-20 wt%, respectively; Fig. 10), but TiO_2 and MgO/FeO_{tot} ratios are low. In the K_2O-silica classification diagram, volcanic rocks straddle the medium and low K series (Fig. 4). They are low in Ni and Cr and have a Co/Ni ratio > 1, indicative of extensive crystallisation of ferromagnesian minerals. Strontium abundances do not correlate with SiO_2, indicating extensive plagioclase crystallisation, contrary to Ba (Fig 11). K_2O/Rb ratios range between 300 and 350, characteristic of the volcanic rocks of the whole Lesser Antilles arc (Gill, 1981). Chondrite-normalized REE patterns of the studied rocks show a slight LREE enrichment with La/Yb ratios around 5 (Davidson et al., 2007). These geochemical characteristics are typical of island-arc calc-alkaline series (Jakes and White, 1972) and have been described for volcanic rocks of the other Lesser Antilles islands.

Geochemical studies have stressed the importance of fractional crystallisation of basaltic magma and magma mixing as mechanisms for the origin of the chemical diversity of Montagne Pelée magmas (Figs. 3, 4, 10, 11; Dupuy et al., 1985; Fichaut et al., 1989a; Smith and Roobol, 1990). Chemical variations within individual eruptions are ascribed to fractional crystallisation (McBirney, 1980; Martel et al., 2006; Pichavant et al., 2002). The presence of gabbroic cumulates demonstrates that crystallisation of mafic magmas takes place in the magma chamber, leading to a wide range of derivative liquids, from basalt to basaltic andesite and from basaltic andesite to dacite once amphibole is fractionating, and even through to rhyolite (Fig. 3, 4, 10).

5.2. Magma origin at depth

There is considerable geochemical variation in volcanic products all along the arc (Brown et al., 1977; MacDonald et al., 2000). Because of the central position of Martinique, the volcanic rocks record the whole history of the arc and could reflect magmatic processes active not only under the island but also along the entire arc. Overall, islands to the north (Saba to Montserrat) produce low-K basalts whereas those in the south (Grenadines and Grenada) comprise medium-K picrites and ankaramites. The islands from Guadeloupe to Grenada are typically composed of medium-K basalt or basaltic-andesite. Comparatively, the mafic magmas sampled by the eruptions at Montagne Pelée are not very primitive (Mg# = 55–60, with Mg # = Mg/(Mg + Fe_{tot})), so little information is provided on their possible connection with clearly mantle-derived melts. The most primitive, near-primary high MgO-basalts erupt from other volcanic centers of the southern part of the Lesser Antilles arc, such as Soufrière, St. Vincent (Mg# ~ 73.5) (Bouvier et al., 2008, 2010; Pichavant and Macdonald, 2007) or Grenada (White et Dupré,1986). Over the 25 Ma volcanic activity of Martinique,

contamination of the mantle source by subducted sediments controlled the compositions of the volcanic rocks. Mafic magmas are generated by partial melting from a mantle wedge similar to, or slightly enriched in high field strength elements (HFSE) relative to the mid-ocean ridge basalt (MORB) source and metasomatized by addition of a fluid phase from the subducting slab (Heath et al., 1998; Macdonald et al., 2000). For the period from 127 ka up to present, all eruptive products show a clear linear U/Th correlation passing through the origin, indicating a common magmatic source at depth (Fig. 11; Labanieh et al., 2010).

The Sr, Nd, Hf and Pb isotopic compositions of Martinique rocks encompass the whole range not only of the entire Lesser Antilles arc but also of all arc lavas, ranging from values close to MORB to almost continental values (Davidson, 1983; 1986; Davidson and Harmon, 1989). Consequently the "continental crust-like" signature of Martinique's magmas which also characterizes also the Lesser Antilles arc, was acquired through contamination of the mantle wedge by subducted sediments, and not by crustal assimilation processes (Labanieh et al., 2010). Martinique is a clear case of the coexistence of both sediment melting and a slab dehydration signature, as a function of the distance from the trench (Labanieh et al., 2012).

Halogen (Cl/Br/I) ratios (except those involving F in rhyolitic melts) measured in erupted clasts are conservative during magma differentiation and degassing: they are thus characteristic of pre-eruptive melts and probably indicative of the more primitive magmas (Balcone-Boissard et al., 2010). These ratios vary from one volcano to another in the Lesser Antilles arc, indicating that halogen fractionation occurred by fluid transfer or mantle source heterogeneities, thus the geochemical signature of Martinique's magmas is inherited from both early mantle contamination and element recycling.

5.3. Chemical evolution through time

No significant variations in whole rock chemical compositions have occurred since the beginning of Montagne Pelée volcanic activity (Figs. 3, 4, 10, 11). During the first stage, before 127 ka, corresponding to the growth of Mont Conil growth, whole rocks were mainly andesites. Le Prêcheur flank collapse had no direct consequence on the subsequent magma compositions emitted between 127 and 36 ka: andesites were dominant, though some basaltic andesites were also present in minor amounts. During the third stage, both andesites and basaltic andesites were present in similar proportions (Figs. 3, 4). The 10 kyrs that immediately followed the last flank collapse were characterized by a major emission of basaltic andesites (referred to as low-silica pumice and "Saint Vincent" episode) with some andesites (referred to as silica-rich pumice), as exemplified also in the U1401 marine core (Fig. 4c). Interestingly, the less differentiated magmas have the same composition as the mafic enclaves identified in the 1929 eruptive products. Volcanic activity then evolved towards the emission of mostly andesites, though basaltic andesites were still present. The last two magmatic eruptions of 1902-1905 and 1929-1932 only emitted high silica andesites, with subordinate dacites (Figs. 3, 4, 10).

Though no mafic magma has been erupted as a lava during the last 25 kyrs, mafic enclaves (51-59 wt % SiO_2; alkali <4.5) are present in some of the 1902 and 1929 products, occurring as ovoidal or spherical enclaves (up to 20 cm in diameter), as mafic droplets (up to 1 cm) in andesites, or as dark components of banded rocks (Gourgaud et al., 1989). The occurrence of such mafic composition as mafic enclaves, mingled/mixed products, or identified through mineralogical tracers (the presence of ubiquitous high-Ca core of plagioclase phenocrysts, high-Ca microlites or Al-rich amphiboles) over the whole eruptive history of the volcano is interpreted as evidence of mafic melt intruding the andesitic reservoir (Bourdier et al., 1985; Fichaut et al., 1989a, 1989b; Gourgaud et al., 1989; Martel et al., 2006; Fig. 12a). In addition, the elevated fO_2 inferred for the Montagne Pelée mafic liquids (NNO)

is consistent with the general view that subduction zone primary basalts are oxidized (Martel et al., 2006, Pichavant et al., 2002).

6. Discussion

6.1. Magma production rate

Wadge (1984) proposed a rough estimation of the volume of magma emitted by all the active volcanoes of the Lesser Antilles arc in the last 100 ka: for Montagne Pelée, the estimated volume of magma erupted for the last 10 and 100 ka is roughly the same (~8 km^3). However, based on the evolution of the paleotopography of Montagne Pelée following a geomorphological model of evolution, an estimated volume for the volcanic edifice built during the first stage (Mont Conil, 550-127 ka) is estimated at 35 km^3, during the second stage (127- 36 ka) at 26.2 km^3, and the third stage (36 ka-present day) at 10.7 km^3 (Germa et al., 2015). Over the last 25 kyrs, the number of eruptions identified on-land (Westercamp and Traineau, 1983 a, b; Michaud Dubuy, 2019) and in the two marine cores (Boudon et al., 2013, Solaro et al., 2020) is 17 Plinian-subPlinian eruptions and of 38 dome-forming eruptions (Fig 7). Considering that the mean emitted volume during a Plinian eruptions is ~0.5 km^3 DRE and not more than 0.2 km^3 DRE for a dome forming eruption, the volume of emitted magma during the last 25 kyrs is ~16 km^3 DRE, which corresponds to a mean magma production rate of 0.6-0.7 km^3/1000 years. Extrapolating this estimate, 54-63 km^3 were emitted during the second stage of activity of Montagne Pelée and 22-25 km^3 during the third stage. During an eruption, a large part of emitted magma is dispersed directly into the sea from the plume for Plinian eruptions and/or by entering into the sea as PDCs. Added to this is the erosion, which

is very active during and following an eruption, since the on-land pyroclastic deposits are not indurated and are thus easily remobilised. Based on the works on the most recent Soufrière Hills eruption on Montserrat, more than 50 % of the pyroclastic products were dispersed into the sea during the eruption (Le Friant et al., 2004). Most of the scoriaceous pyroclastic flows (a few tens of Mm^3) produced by the 1979 explosive eruption of the Soufrière on St. Vincent (Shepherd et al., 1979) were eroded in the year following the eruption (author's observation). Both observations for these two other volcanic islands of the Lesser Antilles support that on Montagne Pelée, the estimated volume of volcanic edifice built during the second and third stages proposed by Germa et al. (2015), of 26.2 and 10.7 km^3 respectively, are consistent with the estimated magma production rate based on chronostratigraphical studies.

6.2. Flank collapses: their key role in the architecture and evolution of Montagne Pelée and the emitted magmas

Flank collapses exert a direct prime control on the volcanic edifice morphology. Montagne Pelée, like the other volcanoes of Martinique (Pitons du Carbet) and of the southern part of the Lesser Antilles arc (Soufrière, St. Lucia or Soufrière, St. Vincent) experienced infrequent but large-volume flank collapses in contrast to volcanoes of the northern part where flank collapses are more frequent but mobilize smaller volumes (Boudon et al., 2007). This particularity is linked to the presence of the back-arc Grenada Basin to the west (Fig. 1a) and the well-marked asymmetry of the eastern and western on-land and submarine flanks: on Montagne Pelée, the slopes are estimated today at 20 % to the west but only 5 % to the east, generating a greater instability of the western flank even though the hydrothermal system is not so developed on this side.

The 127 ka flank collapse of Montagne Pelée was followed by the building of a new edifice inside the horseshoe-shaped structure, with a migration of the vents toward the southwest, emphasizing the asymmetry of the whole volcano and thus favoring new instability in this direction. The second 36 ka flank-collapse destroyed a part of this volcanic edifice, generating a new, smaller horseshoe-shaped structure, of lower extent and nested in the first one, in which a new edifice was built (Fig. 2a).

Flank collapses also have an indirect control on the composition of the subsequent magmas. Before the 36 ka flank collapse, composition of the erupted magmas was andesitic (58-63 wt% SiO_2, bulk density ~ 2.65 $g.cm^{-3}$), whereas most of the immediate post collapse magmas consist of basaltic andesites (52-57 wt% SiO_2, bulk density ~ 2.85 $g.cm^{-3}$). These less differentiated magmas were emitted by abundant explosive eruptions (Figs. 3, 4, 10). These changes in both composition and eruptive style are explained by the decrease in the threshold effect exerted by the volcanic edifice on the magma plumbing system (Pinel and Jaupart, 2000, 2005), allowing less silica-rich and less H_2O-rich and thus denser magmas stored at greater depth to reach the surface (Boudon et al., 2013; Solaro et al., 2020). Though stored within the same transcrustal magma system, the less differentiated magmas would not have been emitted without the flank collapse. These magmas are sometimes associated with more evolved magmas of andesitic composition (Fig. 4c) emitted at the beginning of compositionally zoned eruptions. This is illustrated on-land by two eruptions called Saint Vincent 1 and 2 (SV1 and SV2), dated respectively at ~30 cal ky BP and ~26.8 cal ky BP (Fig 6, 7; Traineau et al., 1983; Bourdier et al., 1985). These eruptions generated abundant on-land low-silica pumice PDCs within and outside the horseshoe-shaped structure in the western valleys for SV1 and the northern valleys for SV2. They began with the emission of andesites (> 60 wt% SiO_2) mixed with less differentiated magmas; however, the proportion of felsic material never exceeded 5% of the total volume emitted during this period. Related offshore

deposits were also identified in turbidite deposits directly covering the previous DAD and they share the same geochemical characteristics (Fig. 4c; Solaro et al., 2020).

Similar effects of flank collapse on the plumbing system also occurred in Pitons du Carbet (Martinique), on Soufrière (St. Lucia) and at Soufriere Hills volcano (Montserrat). For the two first examples, highly crystallised evolved magmas were able to reach the surface generating steep lava domes (Boudon et al., 2013). At Soufriere Hills volcano, basaltic magmas were emitted over a 20 ka period following a landslide that took place around 130 ka, before volcanic activity returned to intermediate silicic magmas similar to those emitted before the flank-collapse. Such effects have also been demonstrated in marine cores from the IODP Expedition 340 (Cassidy et al., 2015).

6.3. The plumbing system beneath Montagne Pelée, architecture and dynamics

The chemical composition of materials erupted by Montagne Pelée has not changed significantly over the past 127 kyrs, except during the period 36-25 ka (Figs. 3, 4, 10). This lack of variation in the physical and chemical conditions of magma storage has been emphasized by experimental petrology (Martel et al., 1998), based on the comparison of natural product compositions from the last eruptions (P1, 1902-1905, 1929-1932; phenocrysts and glass) with experimental product compositions. The magma storage zone tapped during the past 25 kyrs activity of Montagne Pelée is composed of an andesitic magma (61-62 wt % SiO_2, on average) that contains ~35-58 vol. % of phenocrysts : 29-49 vol. % plagioclase, 4-9 vol. % orthopyroxene, 1-2 vol. % magnetite, minor clinopyroxene, ilmenite and apatite, destabilized amphibole and olivine (Westercamp and Mervoyer, 1976; Gourgaud et al., 1989; Martel et al., 1998) embedded in a rhyolitic matrix glass (74-77 wt % SiO_2; Martel et al., 2000). The pre-eruptive storage conditions proposed for this andesitic reservoir are 875±25°C,

200±50 MPa, an oxygen fugacity (fO_2) between 0.4 and 0.8 log unit above the nickel-nickel oxide buffer (NNO), and melt H_2O contents of 5.3-6.3 wt % (Martel et al., 1998). These conditions are close to but outside the stability field of amphibole. The large mineralogical heterogeneities and disequilibrium frequently displayed in these volcanic rocks demonstrate the complexity of the deep-crust and syn-eruptive processes. The pre-eruptive H_2O content has been studied more precisely as a direct indicator of pressure of magma storage zone at the time of entrapment. All melt inclusions are rhyolitic in composition (~74–81 wt% SiO_2 and alkali 4-7 wt%). No systematic correlation exists with the nature (or composition) of the host crystal. Pre-eruptive volatile contents are not available for all eruptions. Pre-eruptive H_2O concentrations range between 4.3 and 7.1 wt % in the P1 Plinian fallout and between 3.0 and 7.8 wt % in the pumice flow (Martel et al., 1998; Cooper et al., 2016), which are compatible with the mean H_2O content estimated by the by-difference method by EPMA of 5.5 wt% (Balcone-Boissard et al., 2010; Martel et al., 1998). In the P1 D-PDC, glass inclusions have H_2O contents of 0.4–7.1 wt % and 2.2–6.9 wt % in the dense pumices, respectively (Martel et al., 1998). For comparison, melt H_2O contents calculated from the plagioclase-melt model of Housh and Luhr (1991) yield values ranging between 1.9 and 5.5 wt % H_2O for the P1 samples (Martel et al.,1998; Balcone-Boissard et al., 2010). Inclusions from the May 8, 1902, 1929 dome, and C-PDC contain low amounts of H_2O (0.9–2.5, <2.6, and <2.0 wt % H_2O, respectively).

Co-eruption of basaltic andesites embedded in andesitic magmas is ubiquitous at Montagne Pelée, such as during the most recent eruptions (e.g. 1929-1932 and 1902-1905 eruptions; Gourgaud et al., 1989) or during the 36-25 kyrs period (Pichavant et al., 2002). The presence of felsic magma at the beginning of these eruptions suggests the existence of differentiated magma within the upper part of a stratified magma reservoir (Pichavant et al.,

2002) or in small, shallow batches of more evolved magmas within a "mushy" plumbing system impacted by the ascent of less differentiated magmas stored at depth. All magma compositions thus coexist simultaneously in the plumbing system below Montagne Pelée and may, through various processes, interact either during magma eruption or within crustal reservoirs (Fig. 12a). Crystallization of mafic liquids probably occurs over a substantial pressure range (4–10 kbar, Arculus and Wills, 1980; Pichavant et al., 2002; Cashman and Sparks 2018). Experimental results on a mafic basaltic andesite at 4 kbar demonstrate that the mafic part of the Montagne Pelée chamber is fed by relatively evolved basaltic liquids (Mg # 55–60). They have high temperatures (1050°C), high melt H_2O contents (>5–6 wt %), and high fO_2 (mostly between 1 and 2 log units above the NNO buffer). Crystallisation of these liquids yields early Ol + Cpx + Mt, followed at decreasing temperatures by assemblages dominated by Plag + Amph, although there is evidence that amphibole crystallisation may have started early, together with Ol and Cpx. Plag crystallised under these conditions are highly calcic. Cpx are Al and Fe^{3+}-rich salites. Amph are pargasitic hornblendes, reproducing the compositions of phenocrysts in mafic lavas and cumulates or mafic enclaves from the third stage. Mafic magmas thus progressively crystallize as a result of the combined effect of (1) elevated magmatic H_2O contents (~5–6 wt %), and (2) heat loss that takes place preferentially through the ''head'' of the mafic magma column with a funnel-type geometry.

The main parameter governing the activity of the superficial reservoir is the flux of mafic magma. The present-day situation, with the majority of eruptions comprising differentiated magmas with only accidental mafic enclaves, is typical of low vertical fluxes of mafic magmas. It is tempting to conclude that mafic magmas may also play a role in the triggering of eruptions (Sparks et al., 1977; Gourgaud et al., 1989; Pallister et al., 1996). However, there is little sign in recent eruption products of significant effects (either thermal or

compositional) caused by the intrusion of mafic magmas. This may indicate that the effect of mafic magmas is dominantly mechanical.

Few glass compositions obtained by EPMA have been described (Bourdier et al., 1985, Fichaut et al., 1989a, 1989b; Martel et al., 1998, 2000; Balcone-Boissard et al., 2010; Balcone-Boissard et al., in prep.). Matrix glasses (P1, 1902, 1929 eruptions) are all rhyolitic (74.0–76.5 wt % SiO_2 and alkali 5-7 wt%), and whatever the eruptive style, they are almost identical to the P1 melt inclusions (Martel et al., 2000; Balcone-Boissard et al., 2010). Matrix glasses from the 1929 products have up to 80 wt % SiO_2, as a result of the high crystallinity of the groundmass in these samples. Less differentiated glasses have been identified but are globally rare and poorly characterized; their occurrence is restricted to the post flank collapse event (Bourdier et al., 1985; Fichaut et al., 1989a, 1989b, Pichavant et al., 2002).

6.3. The Plinian - dome-forming eruption duality

Montagne Pelée is one of the most famous volcanoes worldwide exhibiting alternating Plinian/subPlinian and dome forming eruptions, involving mostly andesitic magmas. This activity characterizes the last 25 kyrs (Fig. 7). Most eruptions involve small volumes of magma (a few tenths of km^3, similar to dome-forming eruptions), but rarely more, except for a few Plinian eruptions such as P3 (1 km^3 DRE). The Plinian eruptions, given the large dispersion of pumice fallout generally covering the flanks of the volcano and even sometimes beyond (eg. P3), produce deposits that can be more often identified and dated on-land, at least in the last 25 kyrs, contrary to their effusive counterpart. The same deposits can be recognized as tephra offshore and dated by tephrochronological studies. Lava domes that grow in the summit area of the volcano are likely to be completely destroyed by the following explosive eruptions. Associated PDC deposits such as C-PDCs which are generally channeled along

valleys are easily eroded or covered by more recent deposits. This is even truer for D-PDC deposits, which cover a greater extent but are not channeled: they are generally of lower thickness and even more quickly eroded. In marine cores, only the ash-clouds associated with C-PDCs are dispersed at sea, but given their low altitude, their orientation and their small extent, they are not systematically present in the cores. Some eruptions, such as P1, are multi-style eruptions, beginning with a dome-forming phase which produced laterally directed explosions immediately followed by a Plinian phase (Villemant and Boudon, 1998, Carazzo et al., 2012).

About 55 eruptions have been recorded for the last 25 kyrs years, (Fig. 7), based on on-land data (Westercamp and Traineau, 1983a, b; Roobol and Smith, 1976; Smith and Roobol, 1990; Michaud-Dubuy, 2019) combined with tephrochronological studies (Boudon et al, 2013; Solaro et al., 2020). One third of the eruptions are Plinian/subPlinian eruptions, whereas the majority (2/3) are dome-forming events, some of them generating superficial laterally directed explosions. Considering the preservation of the on-land deposits, we therefore suppose that the number of lava domes eruptions is significantly underestimated when going back in time. The number of eruptions identified in the last 5 kyrs is probably more representative of the current activity of the volcano in the recent period, with an eruptive frequency of 3-4 magmatic eruptions/1000 years and a ratio of one Plinian eruption for every two or three dome-forming events.

The recent eruptions of Montagne Pelée provide a unique opportunity to discuss an eruptive regime model during the transition from an explosive (Plinian) to an effusive (dome-forming) eruptive style. Petrological and phase-equilibrium experimental studies on recent silicic andesitic magmas demonstrated comparable pre-eruptive conditions for both types of eruption: the transition between Plinian and dome-forming eruptive styles is thus unrelated to systematic variations of H_2O concentrations in the magma storage region, implying that

differences in eruptive style are acquired during magma ascent in the conduit during eruption (Martel et al., 1998). For explosive eruptions, the behaviour of H_2O (and other volatiles such as halogens) during magma ascent and degassing may be modelled assuming equilibrium closed-system degassing, following the perfect gas and the volatile solubility laws. Conversely, the lava dome-forming eruption occurs out of equilibrium, in an open-system degassing mode; this can be modelled knowing the degassing-induced melt microcrystallisation rate (Villemant and Boudon, 1998; Balcone-Boissard et al., 2010). Joint geochemical and textural studies suggest that this explosive–effusive transition may be explained by the evolution from a closed- to an open-system degassing regime in the conduit (Fig.12 b,c). This transition regime is also dependant on the permeability of the conduit wall, as it thought to have been the case for the P1 eruption: during the early lava dome-forming phase, open-system degassing is possible through the permeable conduit walls, but this may change if the walls become impermeable (through silica precipitation for instance).

Multi-style eruptions such as P1 are of course very difficult to detect when going back in time, as it is not easy to confirm the contemporaneity of deposits. Some ^{14}C dates for ash- and pumice and C-PDC deposits showing very close ages could correspond to such cases, but it is difficult to confirm them. In addition, models of degassing budgets for the two eruptive styles show that effusive eruptions are far more efficient at degassing magmas than explosive ones (Balcone-Boissard et al., 2010).

Textural and geochemical investigations of erupted clasts, in particular habitus and composition of plagioclase microlites, also highlight significant discrepancies between these two eruptive styles. The chemical composition of the decompression-induced plagioclase microlites cannot discriminate between the two eruptive styles, as the same compositions (An35-55) are displayed, contrary to their textural features (plagioclase area fraction, number density, and morphologies, Martel and Poussineau, 2007). For instance, pumice clasts emitted

during Plinian eruptions are dominantly microlite-free, but sometimes contain very small dendritic microlites characterized by low area fraction but high and variable number density. Conversely, lava dome groundmass textures, though very complex because a pervasive silica phase is present, show large, tabular microlites, with high area fraction and low number density (Martel et al., 2012; Boudon et al., 2015). To constrain the diversity of lava dome degree of explosivity, such textural investigations are relevant. The whole population of 1929-1932 C-PDC clasts displays very heterogeneous groundmass textures, ranging from nearly microlite-free vesicular clasts to microlite-rich dense clasts, with dominantly low number density and low area fraction of large tabular to skeletal microlites of plagioclase. Conversely, in D-PDC clasts, like those of the 1902 eruption, plagioclase microlites are small, skeletal to dendritic in shape, with high number density and high area fraction (Martel et al., 2000; Martel and Poussineau, 2007).

6.4. Explosivity of dome-forming eruptions from Montagne Pelée: recurrent exceptions, with strong implications for risk mitigation

Over the past 25 kyrs, 38 dome-forming eruptions have occurred on Montagne Pelée producing a lava dome which is in general destroyed only by gravitational collapse of unstable parts. Few of them generated a series of superficial laterally directed explosions, like the most famous 1902-1905 eruption (7 explosions in the first four months of the eruption) or the initial dome-forming phase of the P1 eruption (two explosions at the very beginning) (Fig. 9).

The origin of these explosions has recently been discussed, based upon a textural and geochemical study (vesicularity, microcrystallinity, cristobalite distribution, residual water content, crystal transit times) of clasts produced by key eruptions (among them May 8,1902

and the second explosion of the P1 eruption) (Boudon et al., 2015). Superficial explosion of a growing lava dome may be promoted through porosity reduction caused by both vesicles flattening due to gas escape and syn-eruptive cristobalite precipitation. Both processes generate an impermeable and rigid carapace creating overpressurisation in the inner parts of the growing lava dome by the rapid ascent of undegassed magma batches. The relative thickness of the cristobalite-rich carapace is an inverse function of the external lava dome surface area. Thus, the probability of a superficial lava dome explosion inversely depends on its size. Explosive activity more likely occurs at the onset of the lava dome extrusion. When the size of the lava dome increases, the lava dome generally growths in a very irregular way, especially with a varying extrusion rate, and extrusion phases pass through cooler and therefore more highly crystallized zones. Discontinuities are created inside the lava dome that favor the circulation of fluids and thus reduce the impermeability of the internal parts of the lava dome. No overpressure can occur and the lava dome is destroyed only by gravitational collapses of unstable segments, generating C-PDCs channeled along valley(s) below the lava dome.

Montagne Pelée is able to generate this type of superficial laterally directed explosions frequently. In addition to the 1902 and P1 eruptions, other similar deposits have been identified on the southwestern flank of the volcano as well as on the southern flank, for example the Morne Rouge area (dated at 2750 ± 58 cal BP) and the western flank, where there are two successive D-PDCs (with no erosion between them), undated but stratigraphically located in the post-5000 years period. At least 4 dome-forming eruptions in the recent period, 3 of them in the last 3000 years, have produced laterally directed explosions. While most of the directed explosions affected the southwestern flank of the volcano, some may also affected the southern flank (explosion of August 30, 1902 and of 2750 ± 58 cal BP).

Such events have also occurred on other volcanoes, such as during the 1951 eruption of Mount Lamington, though it is not clear if the laterally directed explosion was generated or not by a flank collapse preceding the explosion (Belousov et al., 2020), the 1915 eruption of Lassen Peak (Eppler, 1987) and the 8 ka eruption of Puy Chopine in the Chaîne des Puys (France), (Boudon et al., 2015).

6. Risk assessment and potential means for the management of a future volcanic crisis

Over the last few decades, our increasing knowledge of the eruptive history of Montagne Pelée, the different eruptive styles and the presence of multi-style eruptions raises questions about the risk assessment of this volcano and the management of a future volcanic crisis. The magmas emitted during the recent period of activity were systematically evolved andesitic magmas coming from the storage area located at about 2 kbar. These emitted magmas, particularly those of the dome forming eruptions, commonly contain mafic enclaves indicating active reinjections from deeper ponding zones containing less evolved magmas. It is likely that these enclaves are also present in pumice fallout and ash and pumice C-PDCs, but are more difficult to identify in these deposits. But the abundance of reverse zonations in the orthopyroxenes of several studied Plinian eruptions (Boudon et al., 2018) confirms a reinjection of a hotter and more mafic magma. We can thus infer that, for most of the eruptions, there is a pre-eruptive reinjection of more mafic magma into the stable andesitic reservoir.

Current studies of intracrystalline diffusion in orthopyroxenes from the last 5 Plinian eruptions (Boudon et al., 2018) indicate that the timescales between readjustment in the

reservoir and the eruptions may accelerate one to two years prior eruption, though active some decades before, but less sustainably and thus less easily recorded by the monitoring network. Such times need to be correlated with geophysical and geochemical precursors, which remain difficult on this volcano as no eruption has occurred for nearly a century now. We can however consider that readjustments, and reinjections into the superficial reservoir, will be associated with geophysical signals (for example seismicity, deformations...) or modifications in the permeability of the superficial part of the volcano inducing geochemical variations (such as T, hydrothermal sources and soil gases…). If this is the case, these observations are of great importance because they will provide during a future eruptive crisis, an estimate of the time that separates the readjustment in the reservoir from the eruption. In addition, the frequency of laterally directed explosions during a dome-forming eruption and their occurrence as soon as the magma arrives at the surface must be seriously considered in the management of a future volcanic crisis. But it is currently difficult to predict an explosive phase during lava-dome forming eruptions, because of the absence of early warning signs occurring early at the beginning of the growth of the lava dome.

On the basis of the past eruptions of the last millennia, a series of scenarios can be proposed in the event of reactivation, including no magmatic eruption. In the historical period two phreatic eruptions (1792 and 1851) and two dome-forming eruptions (1902-1905 and 1929-1932) have occurred. In the last two millennia, 7 magmatic eruptions have occurred including the two historical ones: 2 Plinian eruptions (P2 and P3), 4 dome-forming eruptions and a multi-style dome forming-Plinian eruption (P1). Of these 7 eruptions, two dome-forming eruptions (1902 and P1) generated violent D-PDCs at the beginning of the eruption. All the magmatic eruptions of this period were always preceded by a phreatic phase, confirmed by the presence of phreatic ashes at the base of the magmatic deposits. Different scenarios can be proposed (Fig. 13):

- A phreatic eruption (1792, 1851 type)
- A phreatic phase followed by a dome forming eruption without major explosive events (1929-1932 type)
- A phreatic phase followed by a dome forming eruption beginning with one or more superficial laterally directed explosions (1902-1905 type)
- A phreatic phase followed by a sub-Plinian/Plinian eruption generating pumice fallout from a plume and C-PDCs resulting of the collapse of the plume (P2, P3 type)
- A phreatic phase followed by a dome forming eruption generating violent laterally directed explosions followed by a sub-Plinian/Plinian eruption generating pumice fallout from a plume and C-PDCs resulting from the collapse of the plume (P1 type).

The probabilities of occurrence of these different eruptive styles is difficult to establish considering the difficulty of recognizing, in the geological record, deposits from phreatic events which occurred alone and also fine deposits from violent laterally directed explosion from dome forming events given that they are quickly eroded.

7. Concluding remarks

Montagne Pelée, with its deadly activity over the last century, has raised the issue of the explosivity of dome-forming eruptions. A lot of work has been done on this volcano and particularly on the origin of the D-PDCs that caused the destruction of the cities of St. Pierre and Morne Rouge and the death of 30,000 people. Interpretations have evolved over time, but all these works have shed light on this volcano which, as with most subduction volcanoes, has a complex history over its hundreds of thousands of years of activity, punctuated by large flank-collapses leading to major changes in terms of structure and composition of the emitted

magma. This has led to better constraints on the dynamics of magma storage beneath this volcano. A large part of the volcanic activity is marked by alternating Plinian and dome-forming eruptions, particularly highlighted over the last 25,000 years, which makes this volcano a reference for this type of activity. The unusual feature of this volcano is that it has generated several violent and destructive events linked to dome-forming eruptions. This feature must be taken into account in the event of reactivation of the volcano, especially as these violent and destructive events occurred early on the magmatic eruption not more than a few days after the arrival of the magma at the surface. Therefore detailed monitoring of the activity is necessary for the management of a potential eruptive crisis

Acknowledgements

This review has been possible thanks to the works, and results of numerous scientists from different groups and countries, over more than 40 years, cited throughout the text including the studies, analysis and interpretations of the present authors. This work was supported by the Institut de Physique du Globe de Paris and the Volcanological and Seismological Observatory of Martinique (OVSM) without which it would not have been possible to conduct successive field trips and acquire most of the data. This work was also supported by different research programs of INSU-CNRS (PIRPSEV, PNRN, ACI, Tellus, Artemis), several ANR programs (Risk-Volc-An and the present V-Care) and different cruises from the French oceanographic program (Aguadomar, Caraval) and the IODP Expedition 340 for the marine data. We would like also to warmly thank Michel Pichavant and Guillaume Carazzo, who, with their in-depth knowledge of this volcano from a magmatological and chronostratigraphical point of view, took the time to critically comment on the manuscript.

We also thank Aurélie Germa and an anonymous reviewer for their constructive comments, as well as F. van Wyk de Vries for the English proofreading.

References

Anderson, T., Flett. J.S., 1903. Report on the eruption of the Soufrière of Saint-Vincent in 1902 and on a visit to Montagne Pelée in Martinique. Philos. Trans. R. Soc. London 200, 353-553.

Arculus, R.J., Wills, K.J.A., 1980, The petrology of plutonic blocks and inclusions from the Lesser Antilles island arc, J. Petrol. 21, 743-799.

Aubaud, C., Athanase, J.E., Clouard, V., Barras, A.V., Sedan, O., 2013. A review of historical lahars, floods, and landslides in the Prêcheur river catchment (Montagne Pelée volcano, Martinique island, Lesser Antilles) Bull. Soc. Géol. France 184 (1-2), 137-154.

Balcone-Boissard, H., Villemant, B., Boudon, G., 2010. Behavior of halogens during the degassing of felsic magmas. Geochem. Geophys. Geosyst. 11,Q09005. https://doi.org/10.1029/2010G C003028

Barat, A., 1984. Etude du rôle des eaux souterraines dans le mécanisme des éruptions phréatiques. Application à la Montagne Pelée et à la Soufrière de Guadeloupe. Documents du BRGM 115 BRGM ed. Orléans 205p.

Bardintzeff, J.M., Miskovsky, J.-C., Traineau, H., Westercamp, D., 1989. The recent pumice eruptions of Mt. Pelée volcano, Martinique. Part II: Grain-size studies and modelling of the last Plinian phase P1. In: Boudon G, Gourgaud A (eds): Montagne Pelée. J. Volcanol. Geotherm. Res. 38, 35-48.

Belousov, A., 1995. The Shiveluch volcanic eruption of 12 November 1964: explosive eruption provoked by failure of the edifice. J. Volcanol. Geotherm. Res. 66, 357–365.

Belousov, A., 1996. Pyroclastic deposits of March 30, 1956 directed blast at Bezymianny volcano. Bull. Volcanol. 57, 649–662.

Belousov, A., Belousova, M., Hoblitt, R., Patia H., 2020. The 1951 eruption of Mount Lamington, Papua New Guinea: Devastating directed blast triggered by small-scale edifice failure. J. Volcanol. Geotherm. Res., 401: 106947. DOI: 10.1016/ j.jvolgeores.2020.106947

Boudon, G., Lajoie, J., 1889. The 1902 péléean deposits in the Fort Cemetery of St. Pierre, Martinique: a model for the accumulation of turbulent nuées ardentes. In: Boudon, G., Gourgaud, A. (Eds), Mount Pelée. J. Volcanol. Geotherm. Res. 38, 113-129.

Boudon, G., Bourdier, J.-L., Gourgaud, A., Lajoie, J., 1990. Reply. The May 1902 eruptions of Mount Pelée: high-velocity directed blasts or column-collapse nuées ardentes? J. Volcanol. Geotherm. Res. 43, 363-364.

Boudon, G., Le Friant, A., Villemant, B., Viodé, J.-P., 2005. Martinique. In: Lindsay, J.M., Robertson, R.E.A., Shepherd, J.B., Ali, S. (Eds.), Volcanic Atlas of the Lesser Antilles. Seismic Research Unit, The University of the West Indies, Trinidad and Tobago, WI pp 65–102.

Boudon, G., Le Friant, A., Komorowski, J.-C., Deplus, C., Semet, M.P., 2007. Volcano flank instability in the Lesser Antilles Arc: diversity of scale, processes, and temporal recurrence. J. Geophys. Res. 112, B08205.

Boudon, G., Villemant, B., Le Friant, A., Paterne, M., Cortijo, E., 2013. Role of large flank collapses on magma evolution of volcanoes. Insights from the Lesser Antilles Arc. J.

Volcanol. Geotherm. Res. 263, 224-237. http://dx.doi.org/10.1016/j.jvolgeores 2013.03.009.

Boudon, G., Balcone-Boissard, H., Villemant, B., Morgan, D. J., 2015. What factors control superficial lava dome explosivity? Sci. Rep. 5, 14551. doi:10.1038/srep14551

Boudon, G., Balcone-Boissard, H., Morgan, D. J., 2018. Systematic pre-eruptive dynamic of the magma plumbing system leading to Plinian eruption at Montagne Pelée Martinique (Lesser Antilles), COV 2018, Napoli.

Bourdier, J.-L., Gourgaud, A., Vincent, P.M., 1985. Magma mixing in a main stage of formation of Montagne Pelée: the Saint Vincent-type scoria flow sequence (Martinique, F.W.I.). J. Volcanol. Geotherm. Res. 25, 309-332.

Bourdier, J.-L., Boudon, G., Gourgaud, A., 1989. Stratigraphy of the 1902 and 1929 nuée ardente deposits, Montagne Pelée Martinique. In: Boudon, G., Gourgaud, A. (Eds): Mount Pelée. J. Volcanol. Geotherm. Res. 38, 77-96.

Bouvier, A., Vervoort, J.D., Patchett, P.J., 2008. The Lu–Hf and Sm–Nd isotopic composition of CHUR: constraints from unequilibrated chondrites and implications for the bulk composition of terrestrial planets. Earth Planet. Sci. Lett. 273 (1-2), 48–57.

Bouvier, A.-S., Deloule E., Métrich N., 2010. Fluid Inputs to Magma Sources of St. Vincent and Grenada (Lesser Antilles): New Insights from Trace Elements in Olivine-hosted Melt Inclusions. J. Petrol. 51(8), 1597-1615.

Bouysse, P., Westercamp, D., Andreieff, P., 1990. The Lesser Antilles Island Arc. Proceedings of the Ocean Drilling Program, Part B: Scientific Results 110, 29–44.

Brown, G.M, Holland, J.G, Sigurdsson, H, Tomblin, J.F, Arculus ,R.J., 1977. Geochemistry of the Lesser Antilles volcanic island arc. Geochim. Cosmochim. Acta, 41 (6), 785-801.

Brunet, M., Le Friant, A., Boudon, G., Lafuerza, S., Talling, P., Hornbach, M., Ishizuka, O., Lebas, E., Guyard, H. and IODP Expedition 340 science Party, 2016. Composition, geometry, and emplacement dynamics of a large volcanic island landslide offshore Martinique: From volcano flank-collapse to seafloor sediment failure? Geochem. Geophys. Geosyst. 16, doi:10.1002/2015GC006034.

Carazzo, G., Tait, S., Kaminski, E. & Gardner, J.E., 2012. The recent Plinian explosive activity of Mt. Pelée volcano (Lesser Antilles): The P1 AD 1300 eruption. Bull. Volcanol. 74, 2187–2203. doi 10.1007/s00445-012-0655-4

Carazzo, G., Tait, S., Kaminski, E., 2019. Marginally stable recent Plinian eruptions of Mt. Pelée volcano (Lesser Antilles): The P2 AD 280 eruption. Bull. Volcanol. 81, 1–17.

Carazzo, G., Tait, S., Michaud-Dubuy, A., Fries, A., Kaminski, E., 2020. Transition from stable column to partial collapse during explosive volcanic eruptions: The P3 AD 79 Plinian eruption of Mt Pelée volcano (Lesser Antilles). J. Volcanol. Geotherm. Res. 392, 106764. doi.org/10.1016/j.jvolgeores.2019.106764.

Caricchi, L., Burlini L., Ulmer P., Gerya T., Vassalli M., Papale P., 2007. Non-Newtonian rheology of crystal-bearing magmas and implications for magma ascent dynamics. Earth Planet. Sci. Lett. 264, 402–419.

Caricchi L., Sheldrake T., Blundy J., 2018. Modulation of magmatic processes by CO2 flushing. EPSL 491.

Cashman, K.V., Sparks, R. S. J., Blundy, J. D., 2017. Vertically extensive and unstable magmatic systems: a unified view of igneous processes. Science, 355(6331).

Cassidy, M., Manga, M., Cashman, K., Bachmann, O., 2018. Controls on explosive–effusive volcanic eruption styles. Nature Com. 9, 2839.

Cassidy, M., Watt, S.F.L., Talling, P.J., Palmer, M.R., Edmonds M., Jutzeler, M., Wall-Palmer, D., Manga, M., Coussens, M., Gernon, T., Taylor, R.N., Michalik, A., Inglis, E., Breitkreuz, C., Le Friant, A., Ishizuca, O., Boudon, G., McCanta, M.C., Adachi, T., Hornbach, M.J., Colas, S.L., Endo, D., Fujinawa, A., Kataoka, K.S., Maeno, F., Tamura, Y., Wang, F., Ishizuka, O., and Shipboard Science Party, 2015. Rapid onset of mafic magmatism facilitated by volcanic edifice collapse. Geophys. Res. Lett. 42, 4778–4785, doi:10.1002/2015GL064519.

Charland, A., Lajoie, J., 1989. Characteristics of Pyroclastic Deposits At the Margin of Fond-Canonville, Martinique, And Implications for the transport of the 1902 Nuées Ardentes of Mount Pelée. In: Boudon, G., Gourgaud, A. (Eds), Mount Pelée. J. Volcanol. Geotherm. Res. 38, 97-112.

Christiansen, R.L., Peterson, D.W., 1981. Chronology of the 1980 eruptive activity. In Lipman, P.W., Mullineaux, D.R. (Eds), The 1980 eruption of Mount St. Helens, Washington. U.S. Geol. Survey Prof. Paper 1250, 17-30.

Clouard, V., Athanase, J.E., Arbaud, C., 2013. Physical characteristics and triggering mechanisms of the 2009–2010 landslide crisis at Montagne Pelée volcano, Martinique: implication for erosional processes and debris-flow Hazards Bull. Soc. Géol. (1-2), 155-164.

Cooper, G.F., Davidson, J.P. & Blundy, J.D., 2016. Plutonic xenoliths from Martinique, Lesser Antilles: evidence for open system processes and reactive melt flow in island arc crust. Contrib. Mineral. Petrol. 171, 87. doi.org/10.1007/s00410-016-1299-8

Davidson, J.P., 1983. Lesser Antilles isotopic evidence of the role of subducted sediment in island arc magma genesis. Nature 306, 253–256.

Davidson, J., 1986. Isotopic and trace element constraints on the petrogenesis of subduction-related lavas from Martinique, Lesser Antilles. J. Geophys. Res. 91 (B6), 5943–5962.

Davidson, J., Harmon, R.S., 1989. Oxygen isotope constraints on the petrogenesis of volcanic arc magmas from Martinique, Lesser Antilles. Earth Planet. Sci. Lett. 95, 255–270.

Davidson, J.P., 1987. Crustal contamination versus subduction zone enrichment: example from the lesser antilles and implications for mantle source compositions of island arc volcanic rocks. Geochim. Cosmochim. Acta 51 (8), 2185 -2198 United States.

Davidson,J.P., Turner, S., Handley, H., Macpherson, C., Dosseto, A., 2007. Amphibole 'sponge' in arc crust? Geology 35(9):787–790. doi 10.1130/g23637a.1

Degruyter, W., Bonadonna, C. 2012. Improving on mass flow rate estimates of volcanic eruptions, Geophys. Res. Lett. 39, L16308, doi:10.1029/2012GL052566.

DeMets, C., Gordon, R.G., Argus, D.F., 2010. Geologically current plate motions, Geophys. J. Int. 181(1), 1-80, doi:10.1111/j.1365-246X.2009.04491.x.

Dupuy, C., Dostal, J., Traineau H., 1985. Geochemistry of volcanic rocks of Mt. Pelée, Martinique. J. Volcanol. Geotherm. Res. 26, 147-165.

Du Tertre, J.-B., 1654. Histoire générale des îles Saint-Christophe, de la Guadeloupe, de la Martinique et autres de l'Amérique, Chez Jacques Langlois ... et Emmanuel Langlois ..., 478 p.

Druitt, T.H., Bacon C.R., 1989. Petrology of the zoned calcalkaline magma chamber of Mount Mazama, Crater Lake, Oregon. Contrib. Mineral. Petrol., 101, 245-259.

Eichelberger, J.C., 1995. Silicic volcanism: ascent of viscous magmas from crustal reservoirs. Annual Review of Earth and Planetary Sciences 23, 41–63.

Eppler, D.B., 1987. The May 1915 eruptions of Lassen Peak, II: May 22 volcanic blast effects, sedimentology and stratigraphy of deposits, and characteristics of the blast cloud. J. Volcanol. Geotherm. Res. 31, 65-85.

Fichaut, M., 1986. Magmatologie de la Montagne Pelée (Martinique). Thèse de doctorat, Univ. Bretagne Occidentale, Brest, Bull. P.I.R.P.S.E.V., 120, 320 pp.

Fichaut, M., Maury, R.C., Traineau, H., Westercamp, D., Joron, J.L., Gourgaud, A., Coulon, C., 1989a. Magmatology of Mt Pele´e (Martinique, F.W.I). III, Fractional crystallisation versus magma mixing, J. Volcanol. Geotherm. Res., 38(1-2) 189-213.

Fichaut, M., Marcelot, G., Clocchiatti, R. 1989b. Magmatology of Mt. Pelée (Martinique, F.W.I.). II: petrology of gabbroic and dioritic cumulates. In: Boudon, G., Gourgaud, A. (Eds): Mount Pelée. J. Volcanol. Geotherm. Res. 38, 171-18. https://doi.org/ 10.1016/0377-0273(89)90036-X

Fisher, R.V., Smith, A.L., Roobol, M.J, 1980. Destruction of St. Pierre, Martinique by ash cloud surges, May 8 and20, 1902. Geology 8, 472-476.

Fisher, R.V., Heiken G.F., 1982. Mt Pelée, Martinique: May 8 and20, 1902, Pyroclastic flows and surges. J. Volcano. Geortherm. Res. 13, 339-371.

Germa, A., Quidelleur, X., Labanieh, S., Lahitte, P., Chauvel, C., 2010. The eruptive history of Morne Jacob volcano (Martinique Island, French West Indies): Geochronology, geomorphology and geochemistry of the earliest volcanism in the recent Lesser Antilles arc. J. Volcanol. Geotherm. Res. 198, 297-310.

Germa, A., Quidelleur, X., Lahitte, P., Labanieh, S., Chauvel, C., 2011a. The K–Ar Cassignol-Gillot technique applied towestern Martinique lavas: A record of Lesser Antilles arc activity from 2 Ma to Mount Pelée volcanism. Quaternary Geochronology 6, 341–355.

Germa, A., Quidelleur, X., Labanieh, S., Chauvel, C., Lahitte, P., 2011b. The volcanic evolution of Martinique Island: Insights from K–Ar dating into the Lesser Antilles arc migration since the Oligocene. J. Volcanol. Geotherm. Res. 208, 122-135.

Germa, A., Lahitte, P., Quidelleur, X., 2015. Construction and destruction of Mount Pelée volcano : Volumes and rates constrained from a geomorphological model of evolution. J. Geophys. Res. Earth Surf., 120, 1206-1226, doi :10.1002/2014JF003355.

Gill, J.B., 1981. Orogenic Andesites and Plate Tectonics, Springer-Verlag, NewYork.

Gonnermann, H.M., Manga, M., 2007. The fluid mechanics inside a volcano. Annu. Rev. Fluid Mech. 39, 321–356.

Gourgaud, A., Fichaut, M., Joron, J.L., 1989. Magmatology of Mt. Pelée (Martinique, F.W.I.). I: Magma mixing and triggering of 1902 and 1929 nuées ardentes. In: Boudon G, Gourgaud A (eds): Montagne Pelée. J. Volcanol. Geotherm. Res. 38, 143-169.

Gueugneau, V., Kelfoun K., Charbonnier, S., Germa, A., Carazzo, G. 2020. Dynamic and Impacts of the May 8th, 1902 Pyroclastic Current a Mount Pelée (Martinique): New Insights From Numerical Modeling. Front. Earth Sci. 8:279. doi:10.3389/feart.2020. 00279

Heath, E., Macdonald, R., Belkin, H., Hawkesworth, C., Sigurdsson, H., 1998. Magma genesis at Soufrière volcano, St Vincent, Lesser Antilles arc. J. Petrol. 39, 1721-1764.

Hirn, A., Girardin, N., Viodé, J.-P., Eschenbrenner, S., 1987. Shallow seismicity at Montagne Pelée volcano, Martinique, Lesser Antilles. Bull. Volcanol. 49, 723-728.

Housh, T.B., Luhr, J.F., 1991. Plagioclase-melt equilibria in hydrous systems. Am. Mineral., 76, 477-492.

http://www.ipgp.fr/fr/ovsm/bilans-trimestriels-de-lovsm

Jakes, P., White, A.J.R., 1972. Major- and trace-element abundances in volcanic rocks of orogenic areas. Geol. Soc. Am. Bull., 83, 29-40.

Kopp, H., Weinzierl, W., Becel, A., Charvis, P., Evain, M., Flueh, E.R., Gailler, A., Galve, A., Hirn, A., Kandilarov, A., Klaeschen, D., Laigle, M., Papenberg, C., Planert, L., Roux, E., 2011. Deep structure of the central Lesser Antilles Island Arc: Relevance for the formation of continental crust, Earth Planet. Sci. Lett., 304 (1–2), 121-134.

Labanieh, S., Chauvel, C., Germa, A., Quidelleur, X., Lewin, E., 2010. Isotopic hyperbolas constrain sources and processes under the Lesser Antilles Arc. Earth. Planet. Sci. Lett. 298, 35-46.

Labanieh, S., Chauvel, C., Germa, A., Quidelleur, X., 2012. Martinique: a Clear Case for Sediment Melting and Slab Dehydration as a Function of Distance to the Trench. J. Petrol., 53, 241-2464. doi.org/10.1093/petrology/egs055

Lacroix, A., 1904. La Montagne Pelée et ses Eruptions. Masson ed., Paris, 662 pp.

Lajoie, J., Boudon, G., Bourdier, J.L., 1989. Depositional mechanics of the 1902 pyroclastic nuée ardente deposits of Mount Pelée, Martinique. J. Volcanol. Geotherm. Res. 38, 131-142.

Larue, D.K., Smith, A.L., Schellekens, J.H., 1991. Oceanic island arc stratigraphy in the Caribbean region: don't take it for granite. Sed. Geol. 74, 289–308.

Le Friant, A., Boudon, G., Deplus, C., Villemant, B., 2003. Large scale flank-collapse during the recent activity of Montagne Pelée, Martinique, FWI. J. Geophys. Res. 108, B1, 2055.

Le Friant, A., Lock, E.J., Hart, M.B., Boudon, G., Sparks, R.S.J., Leng, M.J., Smart, C.W., Komorowski, J.-C., Deplus, C., Fisher, J.K., 2008. Late Pleistocene tephrochronology

of marine sediments adjacent to Montserrat, Lesser Antilles volcanic arc. J. Geol. Soc. London165, 279–289.

Le Friant, A. et al., 2015. Submarine record of volcanic island construction and collapse in the Lesser Antilles arc: First scientific drilling of submarine volcanic island landslides by IODP Expedition 340. Geochem. Geophys. Geosyst. 16, 420-442. doi:10.1002/ 2014GC005652.

Legendre, L., Philippon, M., Münch, P., Leticée, J. L., Noury, M., Maincent, G., et al., 2018. Trench bending initiation: Upper plate strain pattern and volcanism. Insights from the Lesser Antilles arc, St. Barthelemy Island, French West Indies. Tectonics, 37, 2777–2797. https://doi.org/10.1029/2017TC004921

Macdonald, R., Hawkesworth, C.J., Heath, E., 2010. The lesser Antilles volcanic chain: A study in arc magmatism. Earth Science Review 49(1),1-76.

Martel, C., Pichavant, M., Bourdier, J. L., Traineau, H., Holtz, F., Scaillet, B., 1998. Magma storage conditions and control of eruption regime in silicic volcanoes: experimental evidence from Mt. Pelée. Earth Planet. Sci. Lett. 156, 89 – 99.

Martel, C., Bourdier, J.-L., Pichavant, M., Traineau, H., 2000. Textures, water content and degassing of silicic andesites from recent Plinian and domeforming eruptions at Mount Pele´e volcano (Martinique, Lesser Antilles arc), J. Volcanol. Geotherm. Res., 96, 191-206.

Martel, C., Poussineau, S., 2007. Diversity of eruptive styles inferred from the microlites of Mt Pelée andesite (Martinique, Lesser Antilles). J. Volcanol. Geotherm. Res, 2007, 166 (3-4), 233-254.

Martel, C., Radadi Ali, A., Poussineau, S., Gourgaud, A., Pichavant, M., 2006. Basalt-inherited microlites in silicic magmas: evidence from Mt. Pelée (Martinique, F.W.I.). Geology 34, 905–908.

Martin-Kaye, P.H.A., 1969. A summary of the geology of the Lesser Antilles. Overseas Geology and Mineral Resources 10(2),172–206.

McBirney A.R., 1980. Mixing and unmixing of magmas. J. Volcanol. Geotherm Res 7, 357–371.

McCulloch, M.T., Gamble, J.A., 1991. Geochemical and geodynamical constraints on subduction zone magmatism. Earth Planet. Sci. Lett. 102, 358–374.

Macdonald, R., Hawkesworth, C.J., Heath, E., 2000. The Lesser Antilles Volcanic chain: a study in arc magmatism, Earth Sci. Rev., 49, 1-76.

Melekhova, E., Schlaphorst, D., Blundy, J., Kendall, J.-M., Connolly, C., McCarthy, A., Arculus, R., 2019. Lateral variation in crustal structure along the Lesser Antilles arc from petrology of crustal xenoliths and seismic receiver functions, Earth and Planetary Science Letters, Volume 516, 12-24, doi.org/10.1016/j.epsl.2019.03.030.

Michaud-Dubuy, A., 2019. Dynamique des éruptions pliniennes : réévaluation de l'aléa volcanique en Martinique. Thèse Université de Paris, 200 pp.

Michaud-Dubuy, A., Carazzo, G., Tait, S., Le Hir, G., Fluteau, F., Kaminski, E., 2019. Impact of wind direction variability on hazard assessment in Martinique (Lesser Antilles): The example of the 13.5 ka cal BP Bellefontaine Plinian eruption of Mount Pelée volcano. J. Volcanol. Geotherm. Res. 381, 193-208. doi.org/10.1016/j.jvolgeores. 2019.06.0040377-0273.

Nagle, F., Stipp, J.J., Fisher, D.E., 1976. K-Ar geochronology of the Limestone Caribbees and Martinique, Lesser Antilles,West Indies. Earth Planet. Sci. Lett. 29, 401-412.

Pallister, J.S., Hoblitt, R.P., Meeker, G.P., Knight, R.J., Siems, D.F., 1996. Magma mixing at Mount Pinatubo: petrographic and chemical evidence from the 1991 deposits, in Fire and Mud, Eruptions and Lahars of Mount Pinatubo, Philippines, edited by C. G. Newhall and R. S. Punongbayan, Univ. of Wash. Press, Seattle, 687-731.

Pichavant, M., Martel, C., Bourdier, J., Scaillet, B. 2002. Physical conditions, structure, and dynamics of a zoned magma chamber: Mount Pelée (Martinique, Lesser Antilles arc). J. Geophys. Res. 107, doi:10.1029/2001JB000315.

Pichot, T., 2012. The Barracuda Ridge and Tiburon Rise, East of the Lesser Antilles (origin, evolution and geodynamic implications). Thèse UBO, http://www.sudoc.fr/17079248X. 287 p.

Perret, F., 1937. The Eruption of Mt. Pelée 1929-1932. Carnegie Inst. Washington, Publ. 458, 126 pp.

Pinel, V., Jaupart, C., 2000. The effect of edifice load on magma ascent beneath a volcano. Phil. Trans. R. Soc. London A358, 1515-1532.

Pinel, V., Jaupart. C., 2005. Some consequences of volcanic edifice destruction for eruption conditions. J. Volcanol. Geotherm. Res. 145, 68-80.

Roobol, M.J., Smith, A.L.,1976. Mount Pelée, Martinique: A pattern of alternating eruptive slyles. Geology 4(9), 521-524.

Samper, A., Quidelleur, X., Boudon, G., Le Friant, A., Komorowski, J.C., 2008. Radiometric dating of three large volume flank collapses in the Lesser Antilles Arc. J. Volcanol. Geoth. Res. 176 (4), 485–492.

Schlaphorst, D., Melekhova, E., Kendall, J.-M., Blundy, J., Latchman, J.L., 2018. Probing layered arc crust in the Lesser Antilles using receiver functions R. Soc. Open Sci., 5, Article 180764, 10.1098/rsos.180764

Shepherd, J.B., Aspinall, W.P., Rowley, K.C., Pereira, J., Sigurdsson, H., Fiske, R.S., Tomblin, J.F., 1979. The eruption of Soufrière volcano, St Vincent April-June 1979. Nature 282, 24-28.

Smith, W.H.F., Sandwell, D.T., 1997. Global sea floor topography from satellite altimetry and ship depth soundings. Science 227, 1956-1962.

Smith, A.L., Roobol, M.J., 1990. Mt Pelée, Martinique; A Study of an Active Island-arc Volcano. Geol. Soc. Am. Memoir 175, 105 p.

Sparks, R.S.J., Sigurdsson, H., Wilson, L., 1977. Magma mixing: A mechanism for triggering acid explosive eruptions, Nature 267, 315-318.

Sparks, R.S.J., Young, S.R., 2002. The eruption of Soufrière Hills Volcano, Montserrat (1995-1999): overview of scientific results. In Druitt, T.H, Kokelaar B.P. (Eds). The eruption of Soufrière Hills Volcano, Montserrat from1995 to 1999. Geological Society, London, Memoirs 21, 45-69.

Speed, R.C., Walker, J.A., 1991. Oceanic-crust of the Grenada Basin in the southern Lesser Antilles arc platform. J. Geophys. Res.-Solid Earth Planets 96 (B3), 3835–3851.

Solaro C., Boudon G., Le Friant A., Balcone-Boissard H., Emmanuel L., Paterne M. and IODP Expedition 340 Science Party (2020). New constraints on recent eruptive history of Montagne Pelée (Lesser Antilles arc) from marine drilling U1401A (340 Expedition IODP). J. Volcanol. Geotherm. Res. doi.org/10.1016/j.jvolgeores.2020.107001

Tanguy, J.-C., 1994. The 1902-1905 eruptions of Montagne Pelée, Martinique: anatomy and retrospection. J. Volcanol. Geotherm. Res. 60, 87-107.

Tanguy, J.-C., 2004. Rapid dome growth at Montagne Pelée during the early stages of the 1902–1905 eruption: a reconstruction from Lacroix's data. Bull. Volcanol. 66, 615-621.

Pichavant, M., Macdonald, R., 2007. Crystallization of primitive basaltic magmas at crustal pressures and genesis of the calc-alkaline igneous suite: Experimental evidence from St Vincent, Lesser Antilles arc. Contrib. Min. Petrol. 154, 535-558.

Traineau, H., 1982. Contribution à l'étude géologique de la Montagne Pelée, Martinique: Evolution de l'activité éruptive au cours de la période récente., Thèse de 3ème cycle,, Univ. Paris XI, Orsay, France.

Traineau, H., Westercamp, D., Coulon, C., 1983. Mélanges magmatiques à la Montagne Pelée (Martinique). Origine des éruptions de type Saint-Vincent. Bull. Volcanol. 46, 243-269.

Traineau, H., Westercamp, D., Bardintzeff, J.-M., Miskovsky, J.-C., 1989. The recent pumice eruptions of Mt. Pelée volcano, Martinique. Part I: Depositional sequences, description of pumiceous deposits. J. Volcanol. Geotherm. Res. 38, 17-33.

Van Soest, M.C., Hilton, D.R., Macpherson, C.G., Mattey, D.P., 2002. Resolving sediment subduction and crustal contamination in the Lesser Antilles arc: a combined He–O– Sr Isotope approach. J. Petrol. 43 (1), 143–170.

Villemant, B, Boudon, G., 1998. Transition between dome-forming and Plinian eruptive styles: H_20 and Cl degassing behaviour. Nature 392, 65-69.

Vincent P.M., Bourdier J.L. and Boudon G., 1989. The primitive volcano of Montagne Pelée: its construction and partial destruction by flank collapse. In G. Boudon and A. Gourgaud (Editors) Montagne Pelée. J. Volcanol. Geotherm. Res., 38, 1-15.

Voight, B., Glicken, H., Janda, R.J., Douglass, P.M., 1981. Catastrophic rockslide avalanche of May 18. In Lipman, P.W., Mullineaux, D.R. (Eds), The 1980 eruption of Mount St. Helens, Washington. U.S. Geol. Survey Prof. Paper 1250, 347-378.

Waitt, R.B., Hansen, V.L., Wood, S. H., 1981. Devastating pyroclastic density flow and attendant air fall of May 18 – Stratigraphy and sedimentology deposits. In Lipman, P.W., Mullineaux, D.R. (Eds), The 1980 eruption of Mount St. Helens, Washington. U.S. Geol. Survey Prof. Paper 1250, 439–460.

Wadge, G., 1984. Comparison of volcanic production rates and subduction rates in the Lesser Antilles and Central America. Geology 12, 555–558. doi.org/10.1130/ 0091-7613

Westercamp, D., Mervoyer, B., 1976. Les séries volcaniques de la Martinique et de la Guadeloupe (FWI). Rapport BRGM-DSCLI, BRGM Orléans.

Westercamp, D., Traineau, H., 1983a. Carte géologique au 1/20 000 de la Montagne Pelée, avec notice explicative. In: B.R.G.M. (Ed.), Orléans.

Westercamp, D., Traineau, H., 1983b. The past 5,000 years of volcanic activity at Mt. Pelee martinique (F.W.I.): implications for assessment of volcanic hazards. J. Volcanol. Geotherm. Res. 17, 159–185. doi.org/10.1016/0377-0273(83)90066-5.

Westercamp, D., Andreieff, P., Bouysse, P., Cottez, S., Battistini, R., 1989. Martinique. Carte géologique à 1/50000. BRGM (Ed.), Orléans, 246 p.

White, W.M., Dupré, P., 1986. Sediment subduction and magma genesis in the Lesser Antilles: isotopic and trace element constraints. J. Geophys. Res. 91, 5927-5941.

Woods, A.W., Koyaguchi, T., 1994. Transitions between explosive and effusive eruptions of silicic magmas. Nature, 370, 641-644.

Zlotnicki, J., Boudon, G., Viodé, J.-P., Delarue, J-F, Mille, A., Bruère, F. 1998. Hydrothermal circulations beneath Montagne Pelée inferred by self potential surveying. Structural and tectonic implications. J. Volcanol. Geotherm. Res., 84, 73-91.

Figures :

Fig. 1. (a) The Lesser Antilles arc (modified from Boudon et al., 2007). Volcanic islands are in black and subaerial coral reef platforms in dark grey. The 100 m depth submarine shelf is light grey. The 500 m and every 1000 m isobaths are shown (predicted bathymetry from Smith and Sandwell, 1997). The dashed lines represent the position of the active and inner arc (in black) and of the older and external arc (in grey). The black arrow and the number indicate the direction and the speed of the subduction. Inset: Martinique SRTM topographic radar map is highlighted (Courtesy of Dr. Ian C.F·Stewart). (b) Swath bathymetry of the west coast of Martinique with the position of the bulge, the submarine landslide deposit (SLD) and the uppermost debris avalanche deposit (DAD). Contour interval is 500 m (modified from Brunet et al., 2015). (c) View of Montagne Pelée from the south.

Fig. 2. (a) Relief Map of Montagne Pelée (DEM from French National Geographic Institute-IGN, resolution 50 m) with the location of the main volcanic edifices and the flank-collapse structures of Montagne Pelée (modified from Le Friant et al., 2003). In grey, the debris avalanche deposits located on land. (b) The hydrographic system of Montagne Pelée. in white ; rivers ; in black : the limit of the flank collapse structure and of the Etang Sec summit crater ; in grey : on-land debris avalanche deposits with hummocky morphology (relief map : Litto 3D from IGN).

Fig. 3. Total alkali-silica (TAS) and AFM diagrams for classification of the Montagne Pelée whole rocks. (a) K_2O+Na_2O-SiO_2 diagram for the whole rocks for the different periods, following the classification of Le Bas et al. (1986). (b) Details on the post 36 ka

period for whole rocks. (c) AFM diagram (Total iron is expressed as Fe_2O_3 (FeO + Fe2O3) synthetizing whole rock data for the 3 stages recognized: blue: Mont Conil, prior to 127 ka and Le Prêcheur flank collapse; red: the period between 127 ka and 36 ka, the second flank collapse event; open circles: the period from 36 ka up to the present day. Black squares: cumulates. Data are calculated on anhydrous basis, with total Fe expressed as Fe2O3. Data are from Traineau et al. 1983; Dupuy et al., 1985; Fichaut, 1986; Bourdier et al., 1989; Smith and Roobol, 1990; Villemant et al., 1996; Pichavant et al., 2002; Davidson and Wilson, 2010; Boudon et al., 2013 and unpublished data from the authors.

Fig 4. K_2O vs. SiO_2 correlation diagram, following the classification of Peccerillo and Taylor (1976). (a) whole rock for the different time periods described in figure 3. (b) Detail of whole rocks of the post 36 ka period, as in figure 3. (c) Glass composition of glass shards from U1401 core (modified from Solaro et al., 2020), for comparison with the whole rock domain (blue box). Tephra : circles (low silica pumice in purple; pumice in orange). Turbidites: diamonds (low silica pumice in pink; pumice in light brown).

Fig. 5. Simplified geological map of Montagne Pelée (modified from Westercamp and Traineau, 1983a). (1) Deposits from the 2nd stage of building (127-36 ka). Deposits from the third stage of building: (2) low silica subPlinian-Plinian eruption (36-25ka); (3) felsic SubPlinian-Plinian eruptions; (4) dome-forming eruptions; (5) recent lava domes; (6) limit of the flank-collapse structures and of the Etang Sec Crater; (7) limit of Montagne Pelée volcano (2nd and 3rd stages).

Fig. 6. Probability domain of calibrated ages (in cal BC) available for Montagne Pelée deposits. (a) the recent period, post 1 cal BP (P3 eruption) ; (b) the period *10 ka - 1 cal BP*; (c) the period *40 - 10 ka cal BP*. Data are from Traineau, 1982; Westercamp and Traineau, 1983a,b; Bourdier et al, 1985, Smith and Roobol, 1990; Michaud-Dubuy, 2019; Carazzo et al., 2020; unpublished data, The ages obtained were calibrated using the free software OxCal (OxCal 4.2, Bronk Ramsey, 2009) with the atmospheric IntCal20 calibration curve, recommended for the Northern Hemisphere (Reimer, 2013). OxCal is a software designed for the analysis of chronological information that we used to calculate the age probability distribution for each dated sample through radiocarbon calibration and, also more specifically here, to analyze groups of ages from stratigraphically-related deposits (i.e., the ages on stratigraphically-constrained samples of the same eruption are validated using the R_Combine function and the χ^2 test prior to calibration) (Ward and Wilson, 1978).

Fig. 7. Frieze showing the evolution of Montagne Pelée and the different volcanic events ; (a) Major events identified throughout the whole evolution of Montagne Pelée; (b) Tephra recorded in the U1401A core (IODP expedition 340), modified from Solaro et al., 2020; (c) Tephra recorded in the CAR-MAR4 core (Caraval Cruise), modified from Boudon al., 2013; (d) Deposits recognized and dated on land during the last 36 ka (Traineau, 1982; Westercamp and Traineau, 1983a,b; Bourdier et al, 1985, Smith and Roobol, 1990; Michaud-Dubuy, 2019; Carazzo et al., 2020.; unpublished data) (e) Synthesis of offshore and on-land data for the last 36 ka; in red, subPlinian and Plinian eruptions, in blue dome-forming eruptions, in green: low-silica pumice-rich eruptions from the period 36-25 ka; events marked by a star, eruptions beginning with a violent laterally directed explosive phase (blue star: dome-forming eruption; red star: Plinian eruption).

Fig. 8. Deposits from different eruptive styles occurring during the recent activity of Montagne Pelée. (a) Succession of Plinian fallout deposits from two recent eruptions (P3 and P1); (b) D-PDCs from the laterally directed explosions occurring during the first dome-forming phase of the P1 eruption. The two D-PDCs cover ochre ash from the phreatic and phreatomagmatic phase and are covered by the pumice fallout from the Plinian phase; (c) pumice fallout from the P1 eruption (1300 years AD); (d) proximal thick pumice fallout deposits from the P1 Plinian eruption; (e) D-PDCs from the laterally directed explosions occurring during the first phase of the 1902- 1905 dome-forming eruption in the Fort Cemetery in the northern part of St Pierre. Three D-PDCs are present: From base to top : May 8 (grey deposit), May 20 (ochre deposit) and June 6 (summit deposit). Black bars in the scale are 5 cm long; (f) Deposits of the May 8 and 20, 1902 D-PDC in a habitation in the city of St Pierre. Black bars in the scale are 5 cm long; (g) The town of St. Pierre after the 1902-1905 eruption. In the background Montagne Pelée and the spine at the top of the lava dome (from Lacroix 1904); (h) View of the summit area of Montagne Pelée with the two lava domes built during the last eruptions of 1902-1905 (in the background) and 1929- 1932 (in the foreground), located inside the Etang Sec caldera. (i) View, from the summit of Montagne Pelée, of the Rivière Blanche valley filled by the 1902-1905 and 1929-1932 C-PDC deposits. (j) Large spine that grew at the top of the lava dome during the 1902-1905 eruption (from Lacroix 1904); (k) C-PDCs from the 1929-1932 dome-forming eruption; (l) megablocks transported in the C-PDC from the 1929-1932 dome-forming eruption.

Fig. 9. Comparative maps showing the distribution of the P1 (a) and May 8, 1902 (b) D-PDC deposits from the laterally directed explosions at the base of the growing lava domes which occurred in the first phase of the eruptions.

Fig. 10. Harker diagrams for Al_2O_3 (a, b), MgO (c,d) and CaO (e,f). Symbols as in figure 3.

Fig. 11 : Trace element correlation diagram. (a) U vs. Th ; (b) Sr vs. SiO2; (c) Ba vs. SiO2; (d) Zr vs. SiO_2; (e) Ce vs La. Symbols as in figure 3.

Fig. 12. The plumbing system beneath Montagne Pelée. (a) schematic view of the plumbing system beneath Montagne Pelée. In blue: mafic magmas; in green basaltic andesitic magmas; in red: andesitic magmas. (b, c) Schematic view of the conduits in the upper part of the volcano: in b, permeable walls of the conduits induces volatile loss from the ascending magma to the surrounding crust generating dome-forming eruptions, in c, impermeable walls of the conduits allow the conservation of gases in the magma and generate subPlinian and Plinian eruptions.

Fig. 13. Possible scenarios for a future eruption on Montagne Pelée. The activity always begins with a phreatic eruption. After the phreatic phase: (a) the activity stops and no magmatic eruption occurs; (b) a dome-forming eruption occurs without violent explosions; (c) a dome-forming eruption occurs and produces violent laterally directed explosions in the first phase of lava dome growth; after this explosive phase, the lava dome grows without violent explosions; (d) a sub-Plinian - Plinian eruption occurs (e) a dome-forming eruption occurs and produces violent laterally directed explosions in the

first phase of lava dome growth; the depressurization of the conduits involved a sub-Plinian – Plinian eruption.

The present authors declare no conflict of interest.

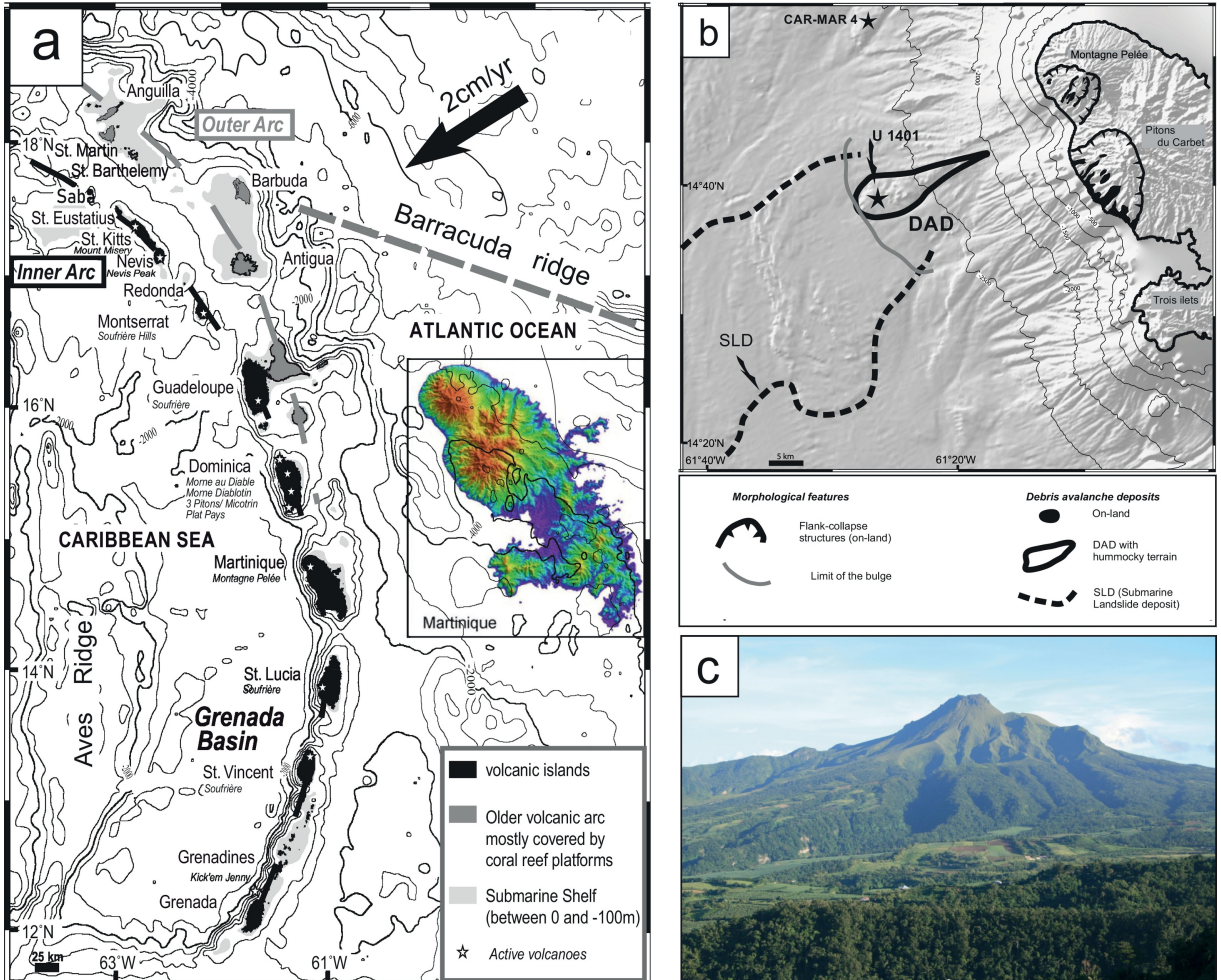
a
Anguilla
Outer Arc
2cm/yr
18°N
St. Martin
St. Barthelemy
Saba
St. Eustatius
St. Kitts
Mount Misery
Nevis
Nevis Peak
Inner Arc
Redonda
Barbuda
Antigua
Barracuda ridge
ATLANTIC OCEAN
Montserrat
Soufrière Hills
Guadeloupe
Soufrière
16°N
Dominica
Morne au Diable
Morne Diablotin
3 Pitons/ Micotrin
Plat Pays
CARIBBEAN SEA
Martinique
Montagne Pelée
Martinique
Aves Ridge
14°N
St. Lucia
Soufrière
Grenada Basin
St. Vincent
Soufrière
Grenadines
Kick'em Jenny
Grenada
12°N
25 km
63°W
61°W
volcanic islands
Older volcanic arc mostly covered by coral reef platforms
Submarine Shelf (between 0 and -100m)
Active volcanoes
b
CAR-MAR 4
Montagne Pelée
Pitons du Carbet
U 1401
14°40'N
DAD
Trois ilets
SLD
14°20'N
61°40'W
5 km
61°20'W
Morphological features
Flank-collapse structures (on-land)
Limit of the bulge
Debris avalanche deposits
On-land
DAD with hummocky terrain
SLD (Submarine Landslide deposit)
c

Figure 1

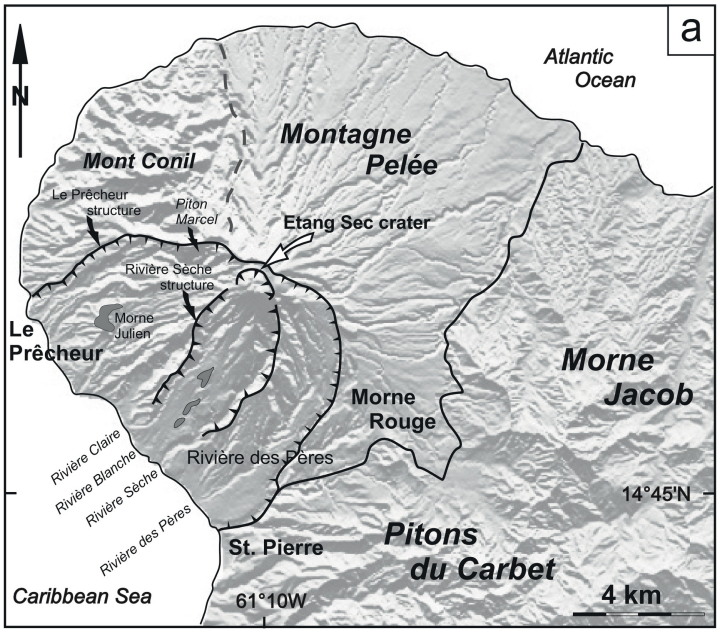
a
N
Atlantic Ocean
Montagne Pelée
Mont Conil
Le Prêcheur structure
Piton Marcel
Etang Sec crater
Rivière Sèche structure
Morne Julien
Le Prêcheur
Morne Jacob
Morne Rouge
Rivière Claire
Rivière Blanche
Rivière Sèche
Rivière des Pères
Rivière des Pères
14°45'N
St. Pierre
Pitons du Carbet
Caribbean Sea
61°10W
4 km

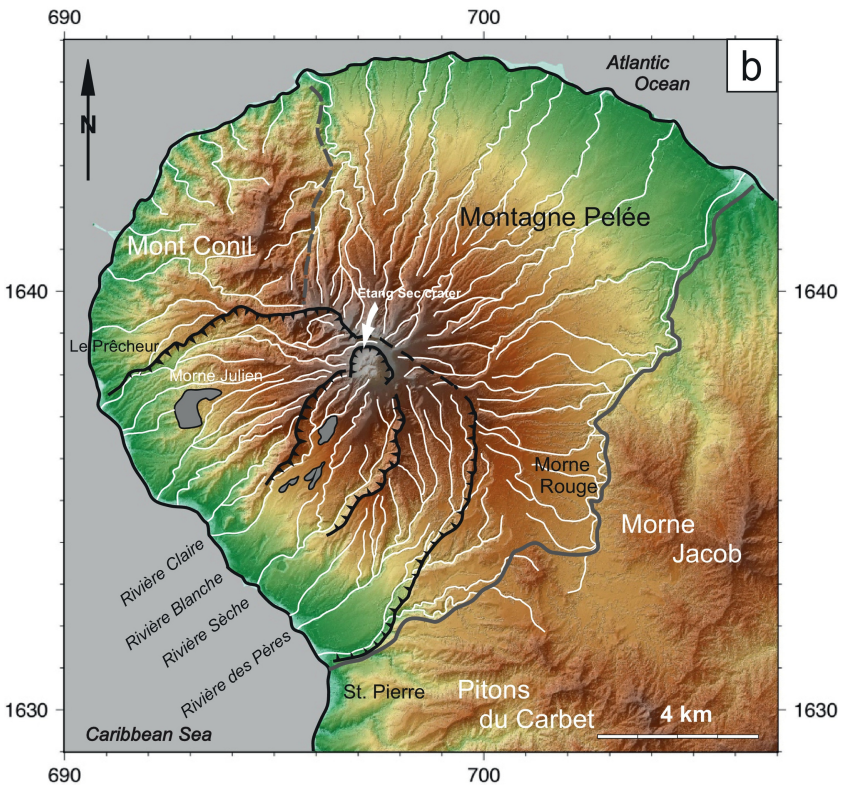
690
700
b
N
Atlantic Ocean
Montagne Pelée
Mont Conil
1640
Etang Sec crater
Le Prêcheur
Morne Julien
Morne Rouge
Morne Jacob
Rivière Claire
Rivière Blanche
Rivière Sèche
Rivière des Pères
St. Pierre
Pitons du Carbet
4 km
1630
Caribbean Sea
690
700

Figure 2

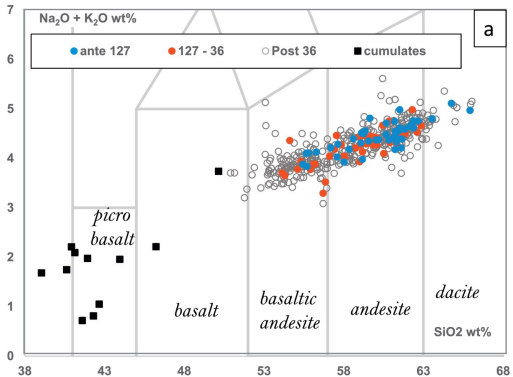
a
Na2O + K2O wt%
ante 127
127 - 36
Post 36
cumulates
picro basalt
basalt
basaltic andesite
andesite
dacite
SiO2 wt%

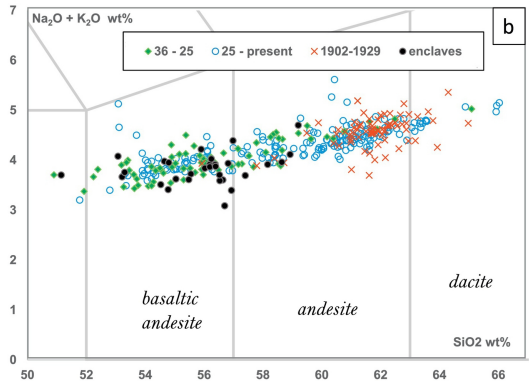
b
Na2O + K2O wt%
36 - 25
25 - present
1902-1929
enclaves
basaltic andesite
andesite
dacite
SiO2 wt%

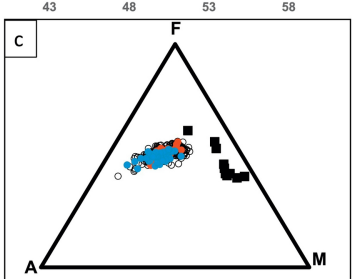
c
F
A
M

Figure 3

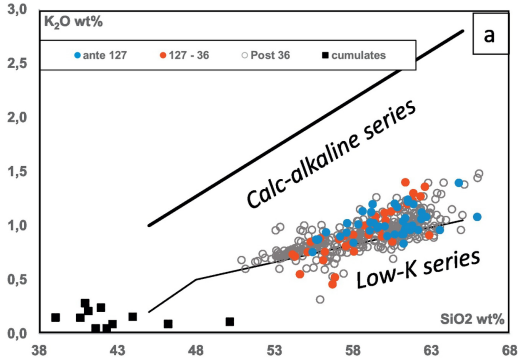
K2O wt%
ante 127
127 - 36
Post 36
cumulates
a
Calc-alkaline series
Low-K series
SiO2 wt%

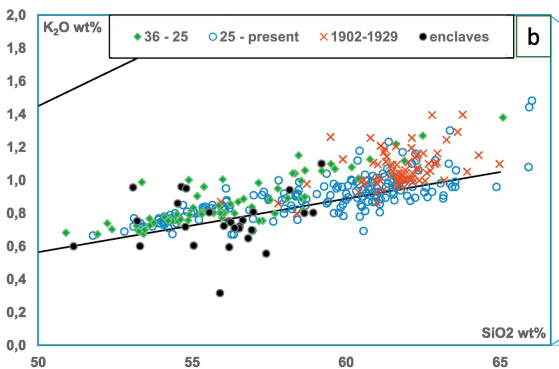
K2O wt%
36 - 25
25 - present
1902-1929
enclaves
b
SiO2 wt%

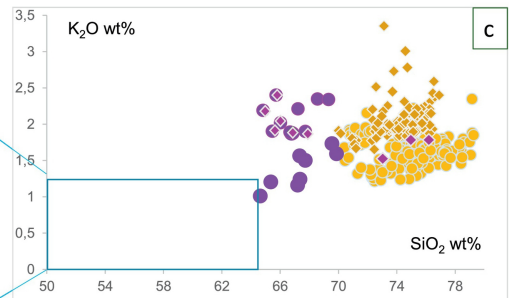
K2O wt%
c
SiO2 wt%

Figure 4

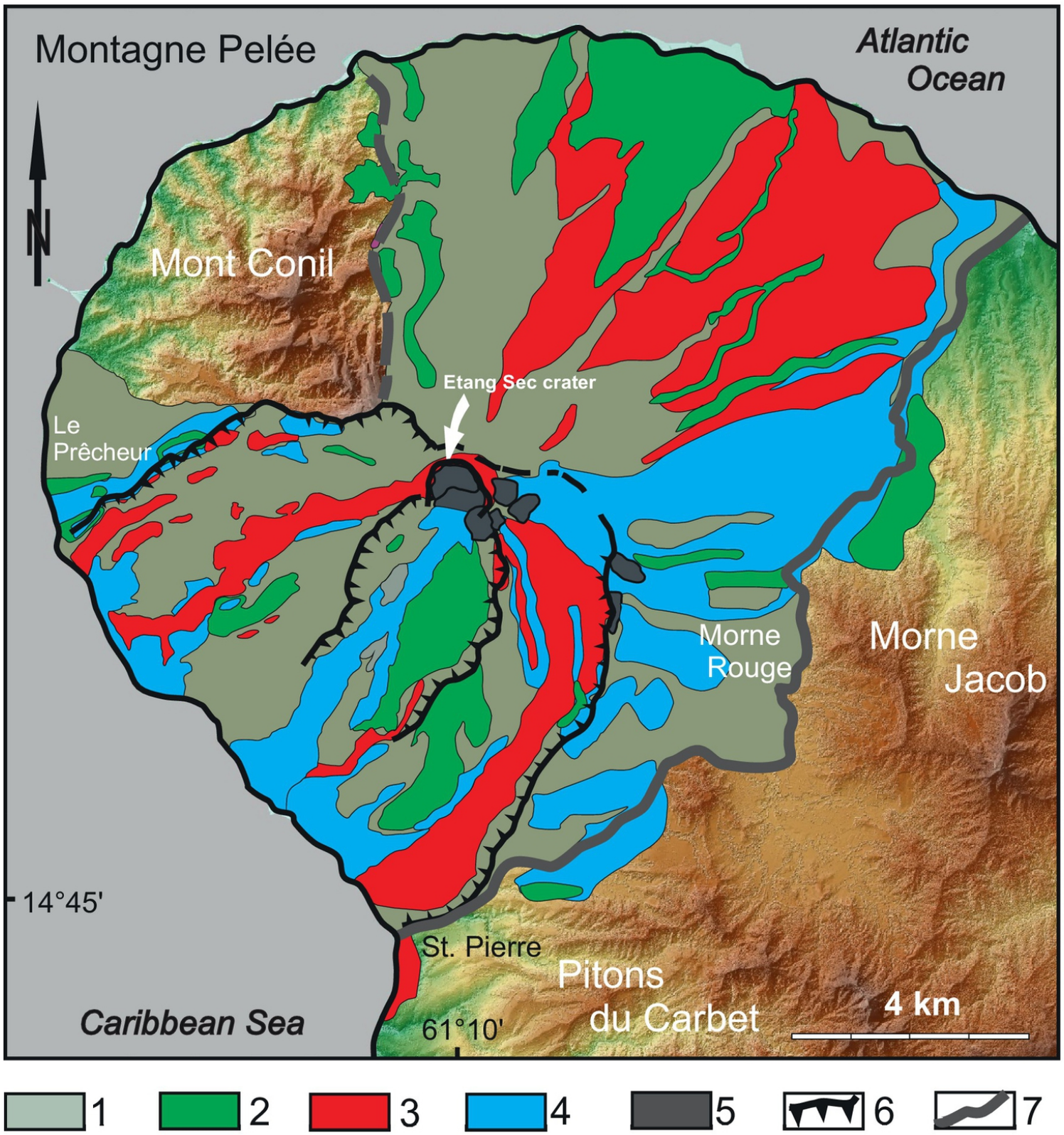
Montagne Pelée
Atlantic Ocean
N
Mont Conil
Etang Sec crater
Le Prêcheur
Morne Rouge
Morne Jacob
14°45'
St. Pierre
Pitons du Carbet
Caribbean Sea
61°10'
4 km
1
2
3
4
5
6
7

Figure 5

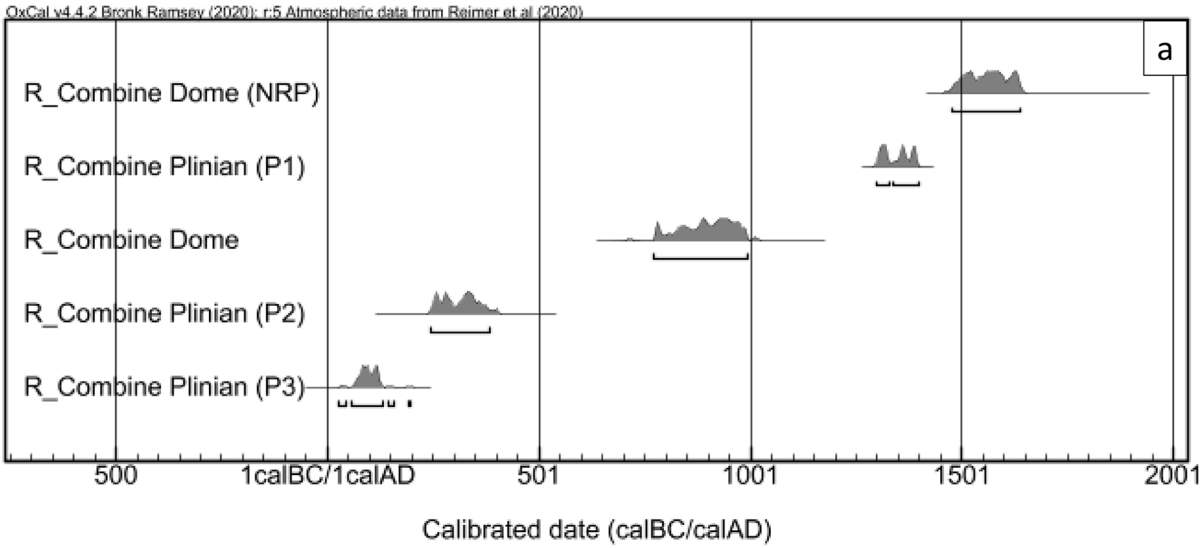
OxCal v4.4.2 Bronk Ramsey (2020); r:5 Atmospheric data from Reimer et al (2020)
a
R_Combine Dome (NRP)
R_Combine Plinian (P1)
R_Combine Dome
R_Combine Plinian (P2)
R_Combine Plinian (P3)
500
1calBC/1calAD
501
1001
1501
2001
Calibrated date (calBC/calAD)

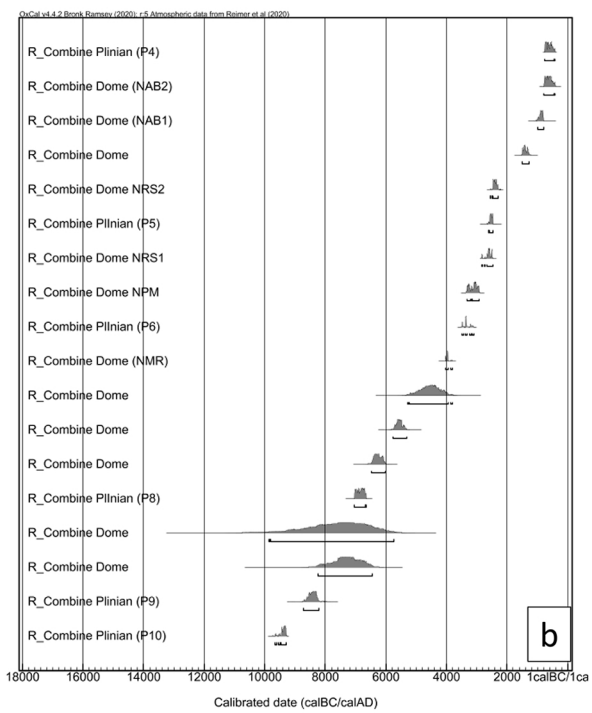
OxCal v4.4.2 Bronk Ramsey (2020); r:5 Atmospheric data from Reimer et al (2020)
R_Combine Plinian (P4)
R_Combine Dome (NAB2)
R_Combine Dome (NAB1)
R_Combine Dome
R_Combine Dome NRS2
R_Combine PlInian (P5)
R_Combine Dome NRS1
R_Combine Dome NPM
R_Combine PlInian (P6)
R_Combine Dome (NMR)
R_Combine Dome
R_Combine Dome
R_Combine Dome
R_Combine PlInian (P8)
R_Combine Dome
R_Combine Dome
R_Combine Plinian (P9)
R_Combine Plinian (P10)
b
18000
16000
14000
12000
10000
8000
6000
4000
2000
1calBC/1ca
Calibrated date (calBC/calAD)

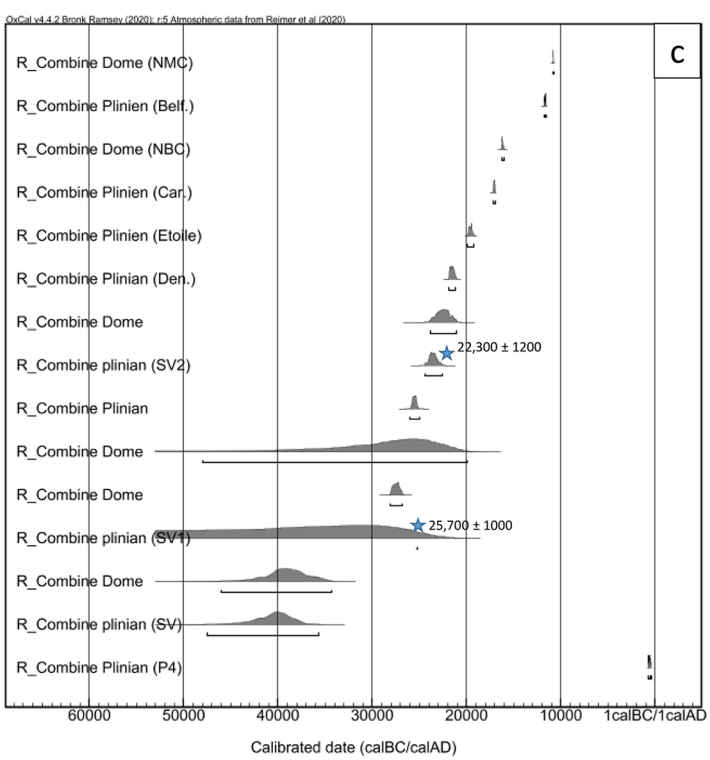
OxCal v4.4.2 Bronk Ramsey (2020); r:5 Atmospheric data from Reimer et al (2020)
c
R_Combine Dome (NMC)
R_Combine Plinien (Belf.)
R_Combine Dome (NBC)
R_Combine Plinien (Car.)
R_Combine Plinien (Etoile)
R_Combine Plinian (Den.)
R_Combine Dome
22,300 ± 1200
R_Combine plinian (SV2)
R_Combine Plinian
R_Combine Dome
R_Combine Dome
25,700 ± 1000
R_Combine plinian (SV1)
R_Combine Dome
R_Combine plinian (SV)
R_Combine Plinian (P4)
60000
50000
40000
30000
20000
10000
1calBC/1calAD
Calibrated date (calBC/calAD)

Figure 6

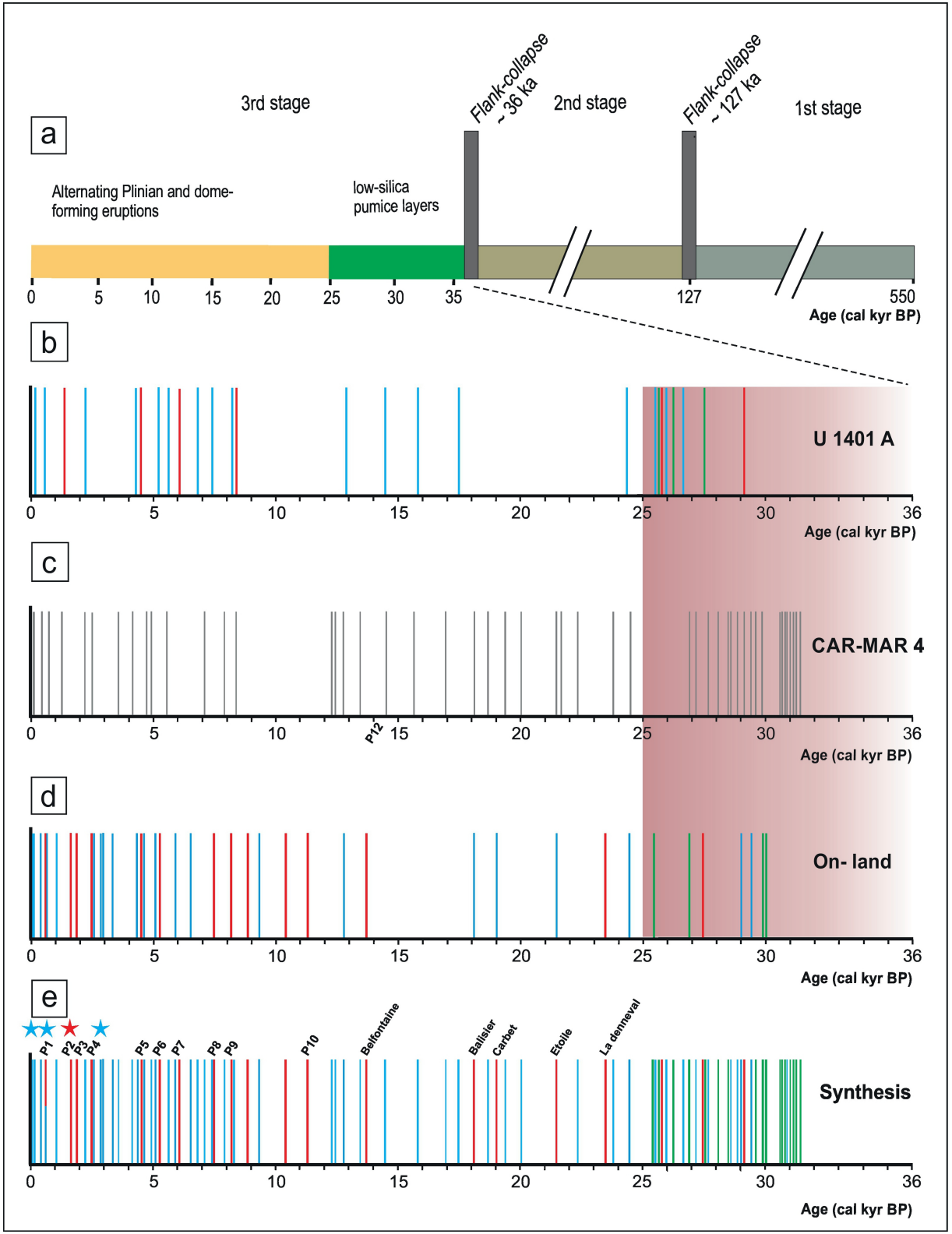
a
3rd stage
Flank-collapse ~ 36 ka
2nd stage
Flank-collapse ~ 127 ka
1st stage
Alternating Plinian and dome-forming eruptions
low-silica pumice layers
0 5 10 15 20 25 30 35 127 550
Age (cal kyr BP)
b
U 1401 A
0 5 10 15 20 25 30 36
Age (cal kyr BP)
c
CAR-MAR 4
0 5 10 P12 15 20 25 30 36
Age (cal kyr BP)
d
On- land
0 5 10 15 20 25 30 36
Age (cal kyr BP)
e
P1 P2 P3 P4 P5 P6 P7 P8 P9 P10 Belfontaine Balisier Carbet Etoile La denneval
Synthesis
0 5 10 15 20 25 30 36
Age (cal kyr BP)

Figure 7

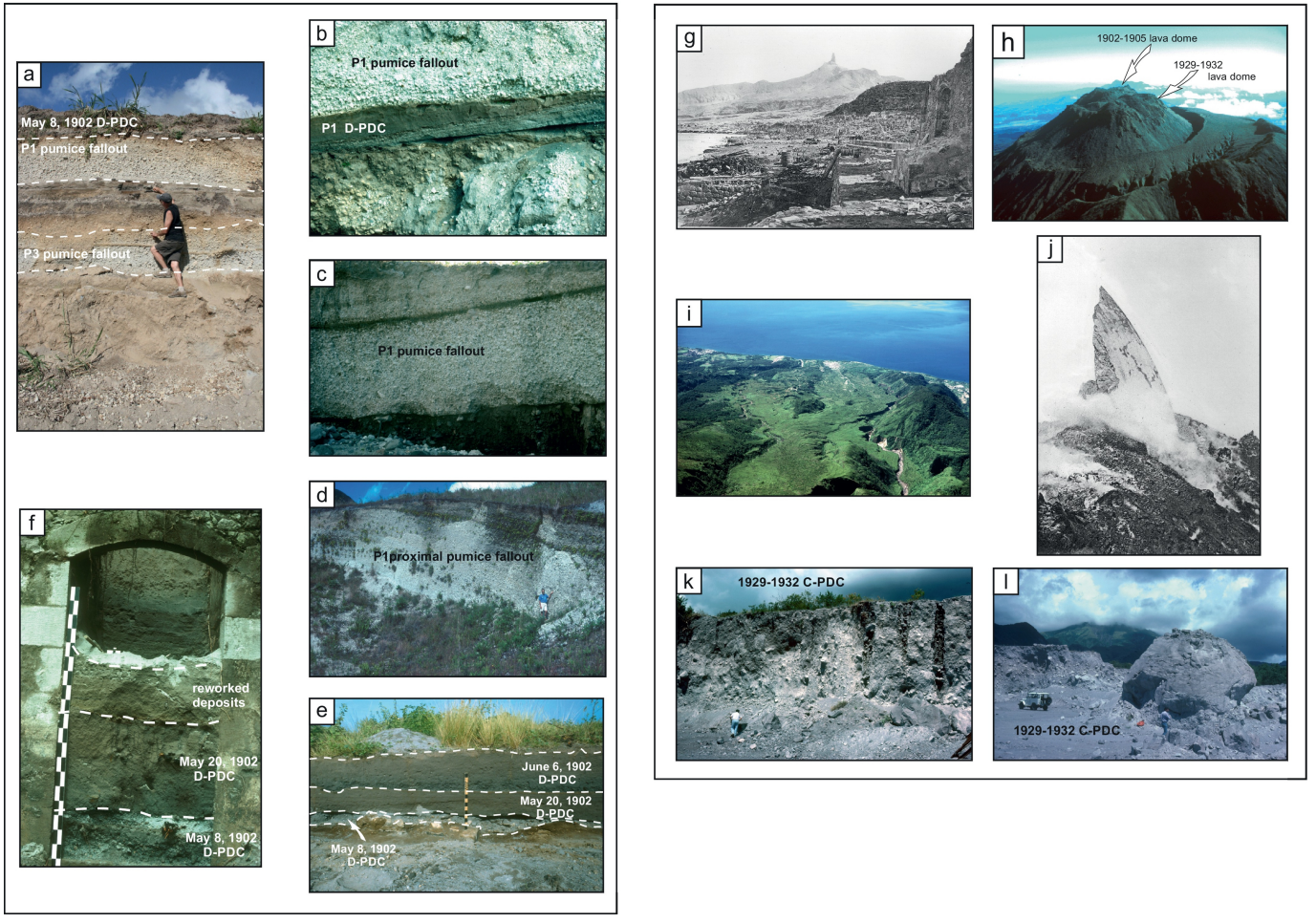
a
May 8, 1902 D-PDC
P1 pumice fallout
P3 pumice fallout
b
P1 pumice fallout
P1 D-PDC
c
P1 pumice fallout
d
P1proximal pumice fallout
e
June 6, 1902 D-PDC
May 20, 1902 D-PDC
May 8, 1902 D-PDC
f
reworked deposits
May 20, 1902 D-PDC
May 8, 1902 D-PDC
g
h
1902-1905 lava dome
1929-1932 lava dome
i
j
k
1929-1932 C-PDC
l
1929-1932 C-PDC

Figure 8

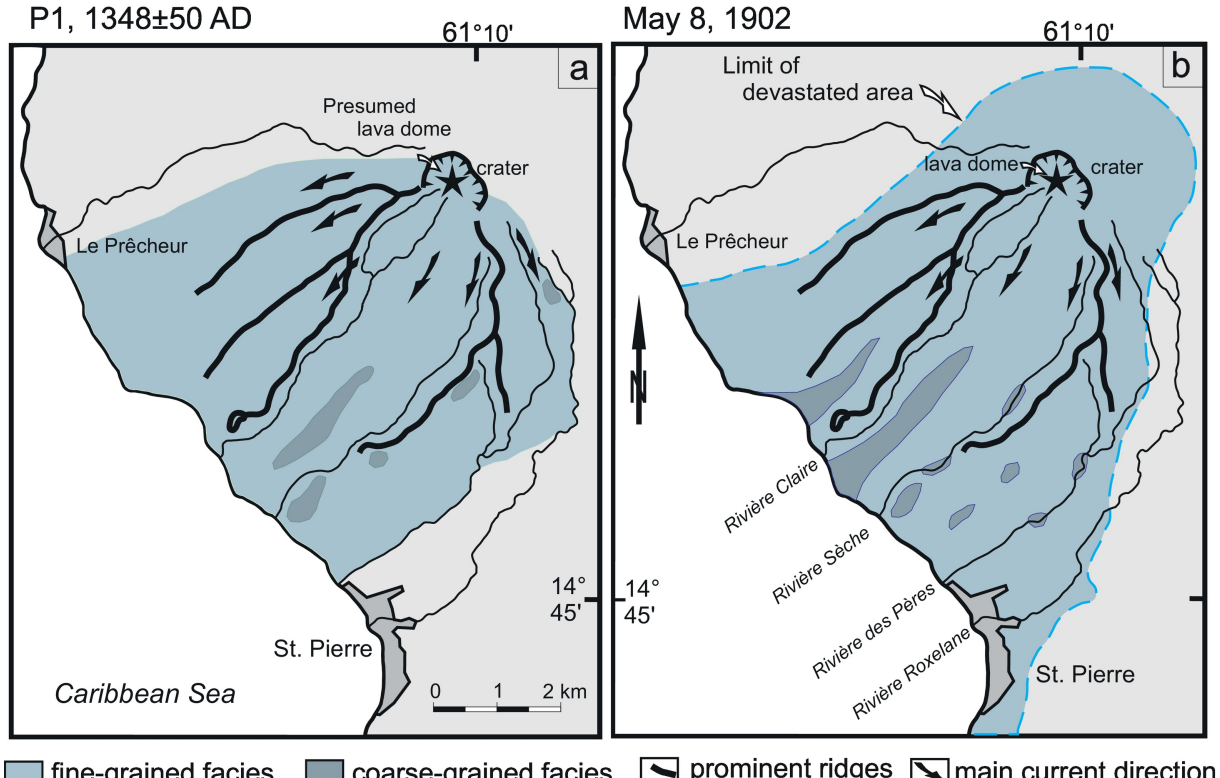
P1, 1348±50 AD
61°10'
a
Presumed
lava dome
crater
Le Prêcheur
14°
45'
St. Pierre
Caribbean Sea
0 1 2 km
May 8, 1902
61°10'
b
Limit of
devastated area
lava dome
crater
Le Prêcheur
N
Rivière Claire
Rivière Sèche
Rivière des Pères
Rivière Roxelane
14°
45'
St. Pierre
fine-grained facies
coarse-grained facies
prominent ridges
main current direction

Figure 9

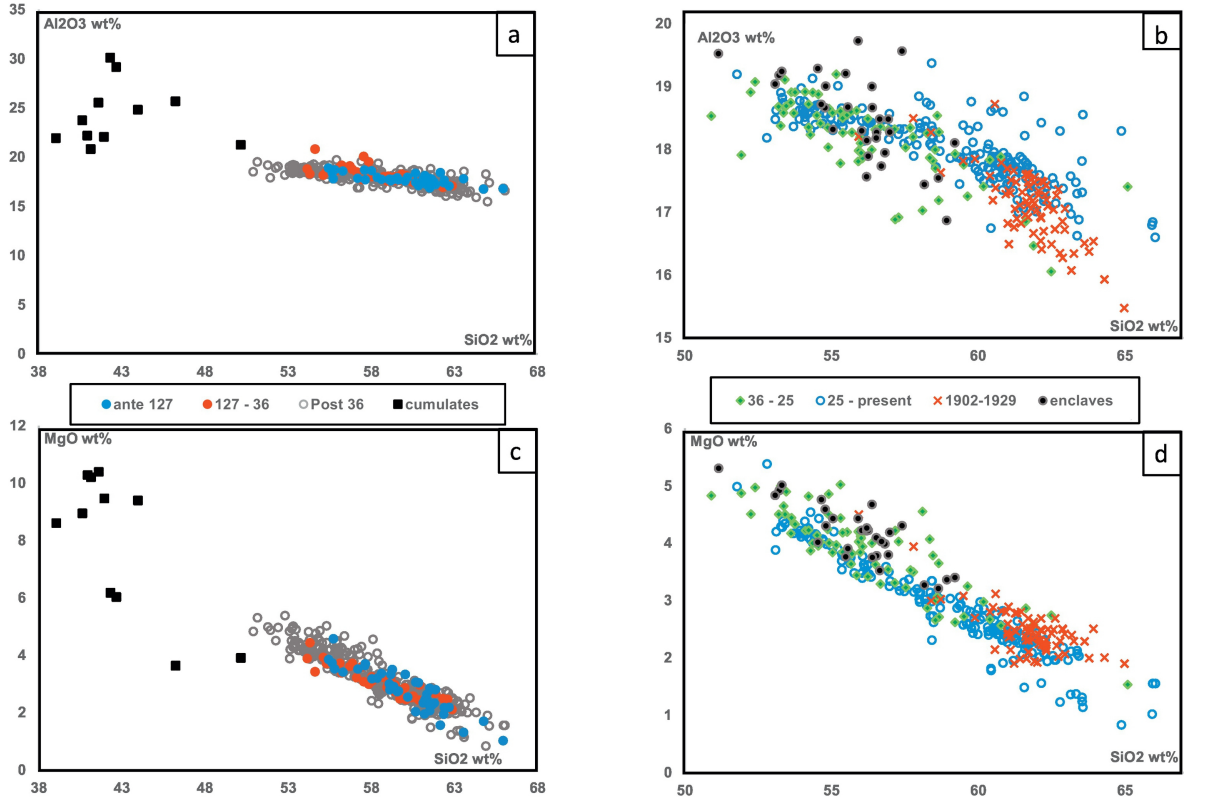
a
Al2O3 wt%
SiO2 wt%
ante 127
127 - 36
Post 36
cumulates
b
Al2O3 wt%
SiO2 wt%
36 - 25
25 - present
1902-1929
enclaves
c
MgO wt%
SiO2 wt%
d
MgO wt%
SiO2 wt%

Figure 10

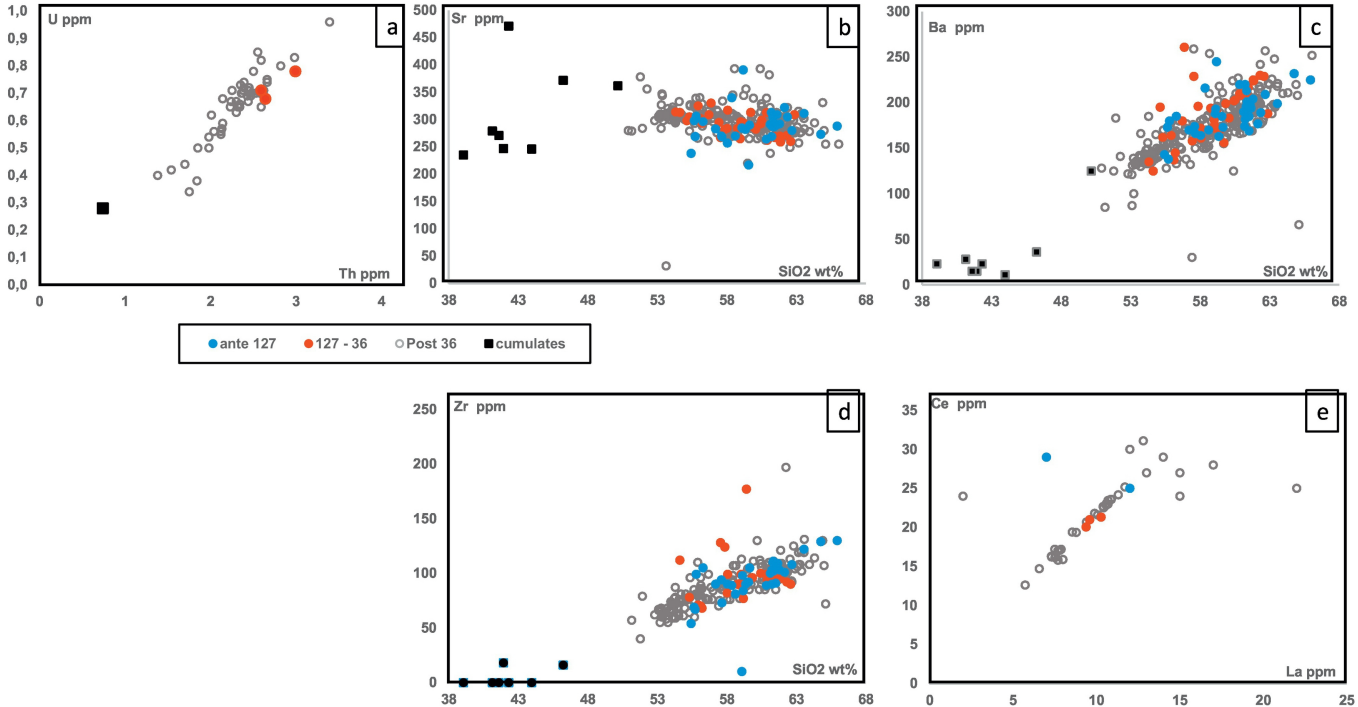
U ppm
a
Th ppm
Sr ppm
b
SiO2 wt%
Ba ppm
c
SiO2 wt%
ante 127
127 - 36
Post 36
cumulates
Zr ppm
d
SiO2 wt%
Ce ppm
e
La ppm

Figure 11

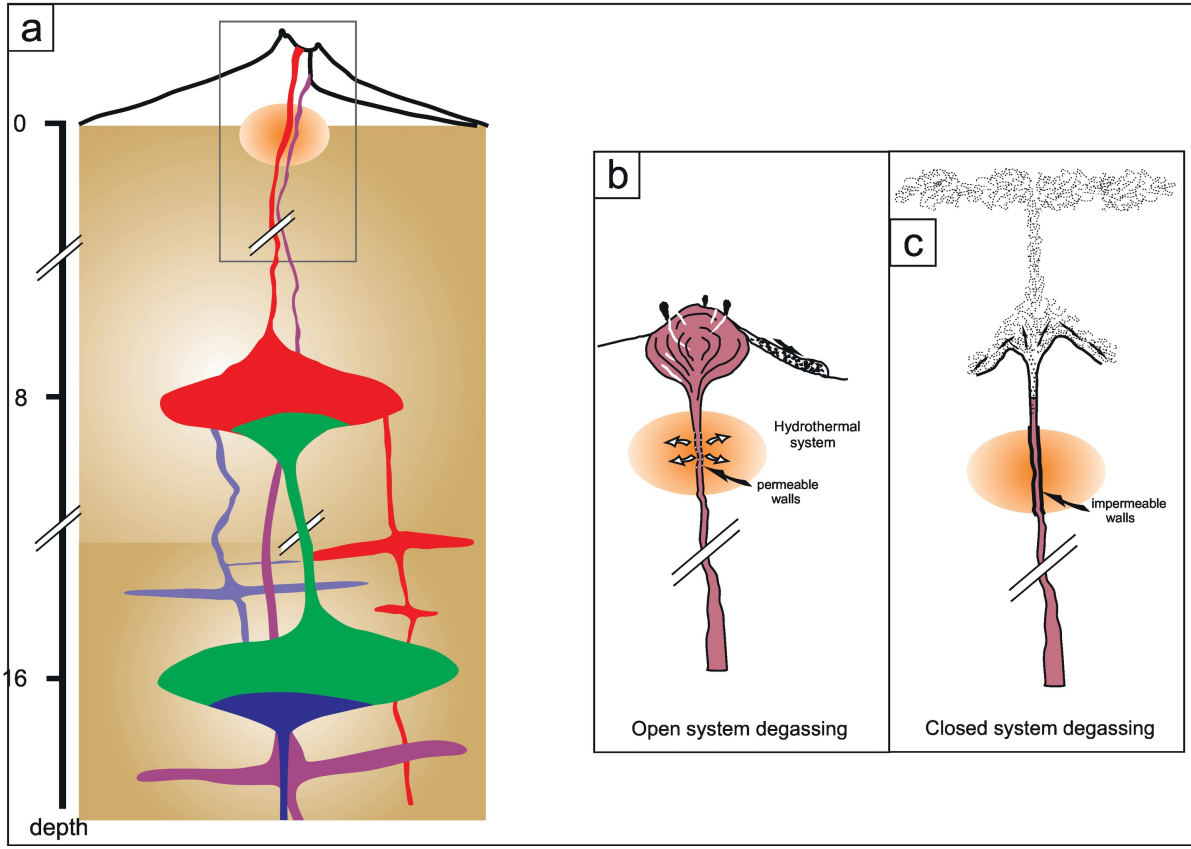
a
0
8
16
depth
b
Hydrothermal system
permeable walls
Open system degassing
c
impermeable walls
Closed system degassing

Figure 12

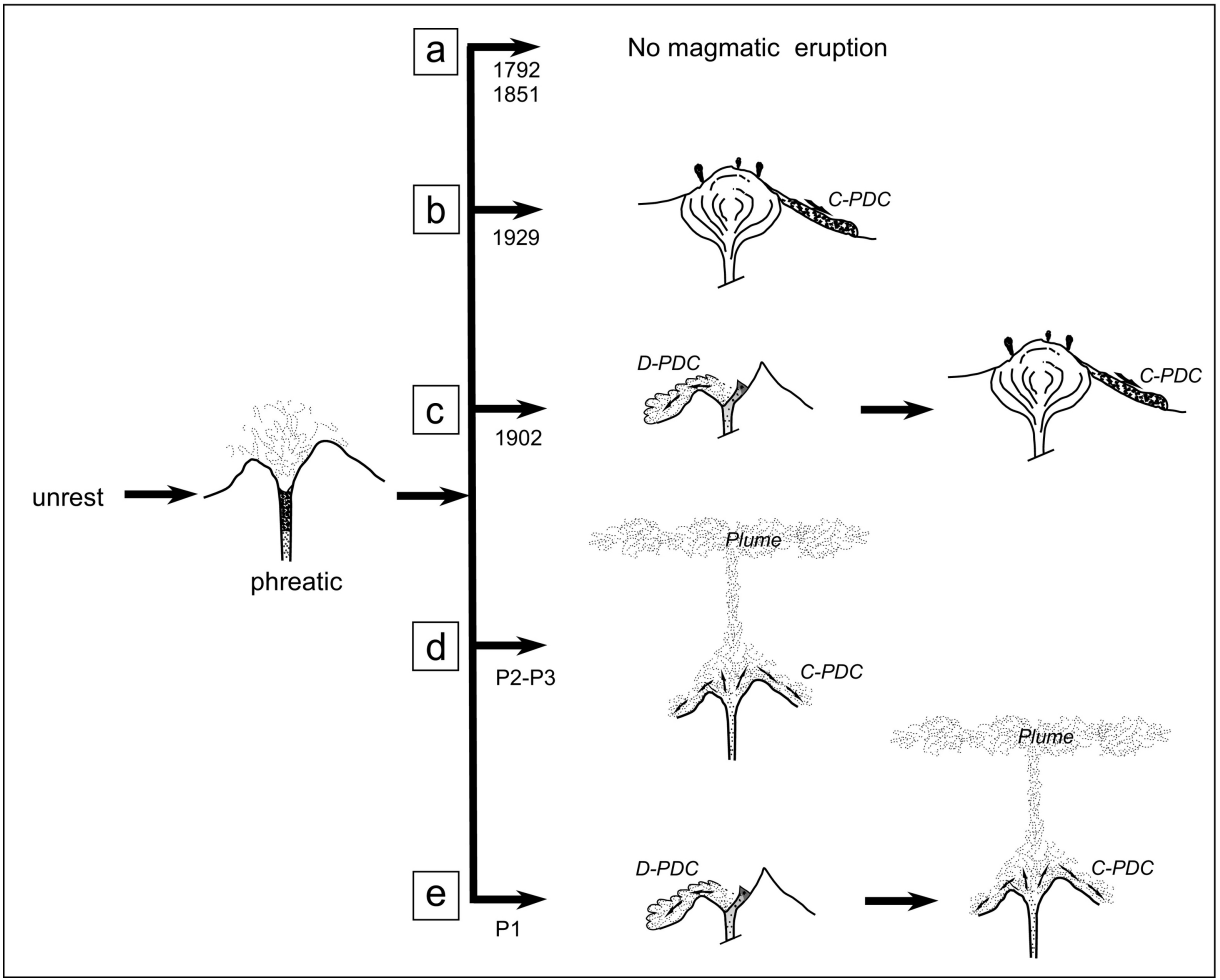
a
1792
1851
No magmatic eruption
b
1929
C-PDC
c
1902
D-PDC
C-PDC
unrest
phreatic
Plume
C-PDC
d
P2-P3
Plume
C-PDC
D-PDC
e
P1

Figure 13